



Centrum výzkumu konkurenční schopnosti české ekonomiky
Research Centre for Competitiveness of Czech Economy

WORKING PAPER No. 1/2009

Sensitivity Analysis of a DSGE model

Jan Čapek, Osvald Vašíček

February 2009



Centrum výzkumu konkurenční schopnosti české ekonomiky
Research Centre for Competitiveness of Czech Economy

Working Papers of the Research Centre for Competitiveness of Czech Economy are issued with support of MŠMT project Rresearch centres 1M0524.

ISSN 1801-4496

Head: prof. Ing. Antonín Slaný, CSc., Lipová 41a, 602 00 Brno,
e-mail: slany@econ.muni.cz, tel.: +420 549491111



Sensitivity Analysis of a DSGE model

Abstract:

This working paper aims at thoroughly analyzing and interpreting results of Marco Ratto's Global (and Local) Sensitivity Analysis (G/LSA) on a particular dynamic stochastic general equilibrium (DSGE) model. The key behavior of the Czech economy is approximated by a Lubik and Schorfheide model, which is a small-scale structural general equilibrium model of a small open economy. The sensitivity analysis class of methods include Stability mapping analysis, Mapping the fit, Reduced form analysis with the use of High dimensional model representation, and Screening with Morris sampling.

Abstrakt:

Tento working paper má za cíl důkladnou analýzu a interpretaci výsledků globální (a lokální) analýzy citlivosti Marca Ratta na konkrétním dynamickém stochastickém modelu všeobecné rovnováhy (DSGE modelu). Klíčové chování české ekonomiky je aproximováno modelem Lubika a Schorfheida, což je malý strukturální model všeobecné rovnováhy popisující malou otevřenou ekonomiku. Třída metod analýzy citlivosti zahrnuje analýzu mapování stability, mapování vyrovnání, analýzu redukováných koeficientů pomocí vícerozměrné modelové reprezentace a prověřovací analýzu s Morrisovým vzorkováním.

Recenzoval:

Contents

Introduction	7
1 Preliminaries	9
1.1 The model	9
1.2 The data	10
1.3 Used software	10
2 Stability mapping	11
2.1 Theory	11
2.2 Results for LS model	12
3 Mapping the fit	14
3.1 Theory	14
3.2 Results for LS model	15
4 High dimensional model representation / Reduced form mapping	19
4.1 Theory	19
4.2 Results for LS model	20
5 Morris sampling / Screening	23
5.1 Theory	23
5.2 Results for LS model	24
Conclusion	26
References	27
A Tables	29
B Figures	32

List of Tables

1	Description of variables and parameters	29
2	Data set and its denotation	30
3	Summary results of stability mapping for different samples	30
4	Detailed results of stability mapping for different samples	30
5	Bi-dimensional projection for best 10 % RMSE	31

List of Figures

1	The data	32
2	Smirnov test for stability analysis 1	33
3	Bi-dimensional projection of parameters driving unacceptable behavior 1	33
4	Smirnov test for stability analysis 2	34
5	Bi-dimensional projection of parameters driving unacceptable behavior 2	34
6	Smirnov test for stability analysis 3	35
7	Bi-dimensional projection of parameters driving unacceptable behavior 3	35
8	CPDs and the distributions of the filtered samples corresponding to the best fit for each singular observed series 1	36
9	CPDs and the distributions of the filtered samples corresponding to the best fit for each singular observed series 2	37
10	CPDs and the distributions of the filtered samples corresponding to the best fit for each singular observed series 3	38
11	CPDs and the distributions of the filtered samples corresponding to the best fit for each singular observed series 4	39
12	Posterior distributions and the distributions of the filtered samples corresponding to the best fit for each singular observed series	40
13	CDFs of the log-prior	41
14	CDFs of the log-likelihood	41

15	CDFs of the log-posterior	42
16	CDFs of the log-prior, log-likelihood and log-posterior 1	43
17	CDFs of the log-prior, log-likelihood and log-posterior 2	44
18	Histograms of the MC sample of the reduced form coefficients	45
19	HDMR of the reduced form coefficient $Y = (\pi_t \text{ vs. } R_{t-1})$	45
20	HDMR of the reduced form coefficient $Y = (\pi_t \text{ vs. } e_{R,t})$	46
21	Ordering of sensitivity indices	46
22	Fit of the reduced form coefficients	46
23	Boxplots of sensitivity indices	47
24	μ_i and σ_i boxplots	48
25	Prior and posterior distributions of the parameters	49
26	Comparison of ordering of sensitivity indices	49

Introduction

This working paper aims at thoroughly analyzing and interpreting results of Marco Ratto's Global (and Local) Sensitivity Analysis (G/LSA) on a particular dynamic stochastic general equilibrium (DSGE) model. This task may need a little explanation and the following paragraphs will therefore introduce the reader to this area of research and will also try to point out its importance.

Sensitivity or robustness analysis has always been an important part of any modeling. Nevertheless, no complex sensitivity analysis in (macro)economic DSGE models was performed until recently. One of the first pioneering works is (Saltelli 2004), which was later updated and extended in (Saltelli 2008). These books introduce a wide variety of tools to analyze sensitivity characteristics of various models. However, these publications are not oriented to economic research, they simply introduce tools for sensitivity analysis for any possible application.

First straightforward application of tools developed in (Saltelli 2004) and (Saltelli 2008) on a macroeconomic DSGE model was published in (Ratto 2008a). This article shed light on many issues, but it simply couldn't cover the whole story within the allotted space. This working paper therefore tries to go into greater detail of the analysis on a single picked case. Completing this task will enable an easier grasp of the G/LSA tool in all further research. More concretely, the researcher will know, what some of the results mean, how the results change under different settings etc.

Section 1 describes the investigated model, the data and the software used in the analyses. The following section titled *Stability mapping* analyses, which parts of domain produce stability, instability or indeterminacy. This analysis unveils possible critical points and flaws of the model itself. Stability mapping doesn't use data so that the results are valid for the set of model equations only.

Section 3 named *Mapping the fit* introduces the data set to the analysis. This section tries to describe the relation between the parameters and the fit of trajectory of observable variables. Since more parameters influence single observable variable and also single parameter influences possibly more observable variables, there may also be some trade-offs. Second part of the section lists most important trade-offs and also offers an explanation to these trade-offs.

The following section explains the so-called *High dimensional model representation* and its use to calculate reduced form coefficients. These coefficients are then used to *Reduced form mapping*. This tool answers questions like: Which parameters are important to a relation between variable A and B? The importance is measured by sensitivity indices – the higher the sensitivity index, the more important the parameter. The section concludes with an overall analysis of sensitivity indices, which reveals the most important parameters in the model as a whole.

Final analytical part, section 5, introduces *Morris sampling*. It is a method to calculate preliminary results, or in another words, it is used for *Screening*. The main advantage of this approach is that it can compute approximate results at very low computational costs.

The following section draws final *Conclusion* and is followed by *References* and appendices: Appendix A contains all tables, appendix B contains all figures.

1 Preliminaries

1.1 The model

This working paper aims at a thorough analysis of a single model, which is a model of (Lubik and Schorfheide 2003)¹

$$y_t = E_t y_{t+1} - [\tau + \alpha(2 - \alpha)(1 - \tau)](R_t - E_t \pi_{t+1}) - \alpha[\tau + \alpha(2 - \alpha)(1 - \tau)]E_t \Delta q_{t+1} - \alpha(2 - \alpha) \frac{1 - \tau}{\tau} \Delta y_{t+1}^* - E_t z_{t+1} \quad (1)$$

$$\pi_t = \beta E_t \pi_{t+1} + \alpha \beta E_t \Delta y_{t+1} - \alpha \Delta q_t + \frac{k}{\tau + \alpha(2 - \alpha)(1 - \tau)} (y_t - \bar{y}_t) \quad (2)$$

$$\pi_t = \Delta e_t + (1 - \alpha) \Delta q_t + \pi_t^* \quad (3)$$

$$R_t = \rho_R R_{t-1} + (1 - \rho_R)(\psi_1 \pi_t + \psi_2 (y_t - \bar{y}_t) + \psi_3 \Delta e_t) + e_{R,t} \quad (4)$$

$$\Delta q_t = \rho_q \Delta q_{t-1} + e_{q,t} \quad (5)$$

$$y_t^* = \rho_{y^*} y_{t-1}^* + e_{y^*,t} \quad (6)$$

$$\pi_t^* = \rho_{\pi^*} \pi_{t-1}^* + e_{\pi^*,t} \quad (7)$$

$$z_t = \rho_z z_{t-1} + e_{z,t} \quad (8)$$

This is a small-scale structural general equilibrium model of a small economy. This working paper uses Czech data set so that model equations (1)–(8) describe elementary behavior of the Czech economy. Due to some difficulties of using Greek letters and sub- and superscripts, somewhat different notation is used in Matlab figures. Explanation of variables and parameters and its notation is in table 1. Generally, Δ denotes first difference so that e. g. $\Delta \xi_t = \xi_t - \xi_{t-1}$, star superscript (*) relates to a foreign economy, subscript t denotes (relative) time and E_t denotes rational expectations made in time t , then e. g. $E_t \xi_{t+1}$ means rational expectations of variable ξ for time $t + 1$ made in time t .

Equation (1) is an open economy IS curve. If $\alpha = 0$, the equation becomes closed economy variant of IS equation. If $\tau = 1$, the world output shocks Δy_{t+1}^* drops out of IS equation and since it is not present in any other equation but AR1 process (6), it drops out of the system completely.

¹Cited from (Ratto 2008a, p. 123) (hereafter LS model). The citation of the model equations is not literal, because sixth equation on page 123 of (Ratto 2008a) is " $y_s = \rho_{y^*} y_{t-1} + e_{y^*,t}$ ", which is obviously an error. Also, in order to prevent confusion, an explanation to variables that have letter e in its notations follows here: e_t in equations (3) and (4) means nominal exchange rate, whereas $e_{.,t}$ in equations (4)–(8) stands for exogenous shocks. Although the notation varies in the number of subscripts, the difference might not be obvious at first glance.

The open economy Phillips curve (2) also collapses to closed economy version if $\alpha = 0$. Consumer price index CPI is introduced in (3) with an assumption of a relative version of purchasing power parity.

Equation (4) is a monetary rule, or in another words, a nominal interest rate equation. It describes, how the monetary authority sets its instrument, when inflation or output depart from their targets or when the currency appreciates or depreciates.

Remaining model equations are just AR1 processes, that describe the course of terms of trade, foreign output and inflation, and technological progress.

1.2 The data

The data span from the first quarter of 1996 to the third quarter of 2008. The source of all data is Czech Statistical Office and are per cent. There are five time series used, their list is in table 2 and they are depicted in figure 1.

1.3 Used software

The main tool used in the analysis is the software package (Dynare). More precisely, the analysis uses one of snapshots of Dynare version 4, which was available at times, when the code was only available via a Subversion server. Recently, Dynare versions 4.0.0–4.0.2 were published as a full release and unfortunately, the analysis doesn't work under these releases. The analysis also requires Global Sensitivity Analysis (hereafter GSA) toolbox by Marco Ratto, which is – according to (Dynare) site – beginning to be added to Dynare version 4. This toolbox used to be downloadable from Euro-area Economy Modelling Centre web pages², but it is unfortunately no longer the case. Documentation for these software packages is semifinished and is in (Griffoli 2007) for Dynare version 4 and in (Ratto 2008b) for GSA.

²<http://eemc.jrc.ec.europa.eu/>

2 Stability mapping

2.1 Theory

Stability mapping helps to detect parameters X_i that are responsible for possible "bad behavior" of the model. First step of the computation is to define two subsets of a full domain: subset B produces behavior (= good behavior of the model), subset \bar{B} produces non-behavior (= bad behavior of the model). What is considered good behavior and what is bad behavior will be concretized later.

N Monte Carlo simulations are then run over the domain, which results in two subsets, $(X_i|B)$ of size n and $(X_i|\bar{B})$ of size \bar{n} , where $n + \bar{n} = N$. The two sub-samples may come from different probability density functions (PDFs) $f_n(X_i|B)$ and $f_{\bar{n}}(X_i|\bar{B})$. Corresponding cumulative distribution functions (CDFs) are $F_n(X_i|B)$ and $F_{\bar{n}}(X_i|\bar{B})$.

If $F_n(X_i|B)$ and $F_{\bar{n}}(X_i|\bar{B})$ differ for a given parameter X_i , the parameter may drive bad behavior of the model if its value falls within \bar{B} subset. The shape of $F_{\bar{n}}(X_i|\bar{B})$ indicates, whether rather smaller or higher values of X_i drive the non-behavior. If the non-behavior CDF is to the left from behavior CDF, it indicates that rather smaller values of X_i are more likely to drive non-behavior. On the other hand, if the non-behavior CDF is to the right from the behavior CDF, it suggests that rather bigger values of X_i drive non-behavior.

In order to obtain also numerical results, a statistic that computes the greatest distance between behavior and non-behavior CDFs is computed. More formally, the (so-called) Smirnov d statistic is defined as

$$d_{n,\bar{n}}(X_i) = \sup ||F_n(X_i|B) - F_{\bar{n}}(X_i|\bar{B})||$$

The Smirnov d statistic has a domain $[0, 1]$, where 0 means that the two (behavior and non-behavior) CDFs perfectly overlap and 1 means that the two underlying subsets B and \bar{B} have no common elements. In other words, $d = 1$ means that one of the CDFs reaches unity before the other increases from zero.

The Smirnov d statistic can also be used to test hypotheses. The question of the hypotheses testing is : "At what significance level p does the computed value of d determine the rejection of the null hypothesis $F_n(X_i|B) = F_{\bar{n}}(X_i|\bar{B})$?" The newly introduced significance level p is often referred to as " p -value" and this working paper also uses this terminology.

Low value of p means that even for – say – 1%, .01% or even values as low as $10^{-100}\%$,

we reject the null that the two CDFs are identical. High value of p means that even for significance levels like 99.5% or 99.9999% we cannot reject the null. If p equals one, we cannot reject the null at any significance level (or, strictly speaking, we can reject the null at significance level 1).³

Results for LS model can be found in figures 2, 4 and 6. The non-behavior subset \bar{B} is defined as a violation of Blanchard-Kahn condition (or – generally – any situation where steady state solution cannot be found). The remaining part of the domain - B - is behavioral. Solid lines in figures 2, 4 and 6 represent CDFs for non-behavioral \bar{B} subset, dotted lines are CDFs for behavioral B subset. Each panel have a `p-value` computed above it.

Bi-dimensional projections are drawn in order to visualize the influence of parameters with high d . In general, a correlation coefficient ρ_{ij} is computed for all couples of parameters and those that exceed (in absolute value) given threshold, are then drawn. Results for the LS model are in figures 3, 5 and 7 with a threshold set to 0.3. Bi-dimensional projections of parameters X_i and X_j where $|\rho_{ij}| > 0.3$ are therefore drawn. A title of each panel is labeled `cc`, which stands for a correlation coefficient ρ_{ij} of the two parameters.

2.2 Results for LS model

Summary numerical results for LS model are in table 3 and detailed numerical results are in table 4. Graphical results are in two kinds of schemes, these are graphs of Smirnov tests 2, 4 and 6 and bi-dimensional projections 3, 5 and 7. Smirnov test graphs are interpreted together with numerical results, bi-dimensional graphs are explained afterwards.

First experiment uses uniform sampling from prior ranges with default number of samples 2,048. Results for this setting are in the second row of table 3, second column of table 4, and figure 2. This graph with Smirnov tests looks similar to Ratto's result⁴. Both figures clearly depict that unacceptable behavior is driven by parameters ψ_1 and ψ_3 . In another words, in cases of both parameters, the solid line is to the left from the dotted line so that

³Computation utilizes Matlab function `kstest2`. Extract from (Matlab documentation): `h = kstest2(x1,x2)` performs a two-sample Kolmogorov-Smirnov test to compare the distributions of the values in the two data vectors `x1` and `x2`. The null hypothesis is that `x1` and `x2` are from the same continuous distribution. The alternative hypothesis is that they are from different continuous distributions. `[h,p,ks2stat] = kstest2(...)` also returns the p-value `p` and the test statistic `ks2stat`. (<http://www.mathworks.com/access/helpdesk/help/toolbox/stats/kstest2.html>)

⁴(Ratto 2008a, p. 124).

rather smaller values of these parameters drive the unacceptable behavior. A more careful look reveals that the domain for unacceptable behavior is for both parameters from zero to one.

Second setting of stability mapping for LS model just adds some 8,000 more samples. Results for Smirnov tests are in the third row of table 3, third column of table 4, and in figure 4 and are virtually the same as for the smaller sample. However, the figure shows that the CDFs are smoother, which is due to the larger sample. Another obvious consequence of increasing the number of samples is an increase in the power of statistical tests. p -values of parameters with already low p -value like e. g. ψ_1 and ψ_3 tend even closer to zero. More concretely, p -value statistics of parameters ψ_1 and ψ_2 get approximately five times closer to zero ($2.6 \cdot 10^{-43} \rightarrow 2.4 \cdot 10^{-213}$ and $2.6 \cdot 10^{-20} \rightarrow 1.4 \cdot 10^{-98}$ respectively). On the other hand, p -values that are already high tend even higher. Examples of parameters with elevated p -values are ρ_{π^*} ($0.991 \rightarrow 1$), rr ($0.891 \rightarrow 0.996$), or ρ_q ($0.631 \rightarrow 0.961$).

Third setting tries to draw priors not from uniform distribution (like Ratto's paper), but from prior distributions defined as in the LS paper⁵. The shape of the CDFs in figure 6 therefore changes, but the results are similar. However, some insignificant differences arise. These concern parameters ψ_3 and τ : Smirnov d statistic for ψ_3 drops from 0.61 to 0.28 and p -value of τ jumps from 0.44 to 0.94. Also, results in last row of table 3 indicate that the part of domain attributed to indeterminacy is larger by almost 2 percentage points. Bi-dimensional projection of the baseline setting (uniform priors, 2,048 samples) plots 3 panels unlike Ratto's one. This is probably due to a differently chosen threshold, Ratto used 0.4 and I used 0.3. However, that rules out just the third panel with $cc=0.31$. The panel with a projection of parameters k and τ has a correlation still slightly above the Ratto's threshold 0.4. The occurrence of this panel can be attributed to a different calibration of the parameters, especially parameter k has quite different calibration⁶. Larger sample of 10,000 draws (in fig. 5) leaves only one panel with a projection of parameters ψ_1 and ψ_3 . This result is in accordance with Ratto's paper. The dots in figures 3 and 5 form a triangle with sides $[0, 1]$ on both parameters ψ_1 and ψ_3 . The correlation of the parameters is approximately $-\frac{1}{2}$. Because the dots represent non-behavior (more concretely – indeterminacy), this leads to the result that behavior requires $\psi_1 + \psi_3 > 1$,

⁵(Lubik and Schorfheide 2003) and also (Ratto 2008a, p. 125)

⁶(Ratto 2008a, p. 125): $\mu = .5, \sigma = .25$, this study sets $\mu = 2, \sigma = .4$.

which is by Ratto's paper called a "generalised Taylor principle". Third setting (prior distributions with 10,000 samples) makes figure 7 hardly useful. The shape is similar to figure 5, but the borderlines are not apparent. However, the correlation coefficient is also cca -.5. Probably because the third setting with prior distributions offers less useful results in comparison with uniform priors, it is not used in Ratto's paper.

This analysis doesn't use data, so the results are just a matter of model relations (equations) and parameter calibration, not the data itself.

3 Mapping the fit

3.1 Theory

Since DSGE models consist of a number of observed variables, which should fit the data as well as possible, mapping the fit may be a useful tool to learn about the linkages that drive the fit of trajectories of particular variables to data. Information provided by the results of mapping the fit can be used to unveil possible trade-offs and maybe also amend model structure or calibrate parameters properly in order to increase the fit of variables of interest.

The procedure is carried out as follows:

1. Structural parameters are sampled from posterior distribution,
2. RMSE⁷ of 1-step-ahead prediction is computed for each of observed series,
3. 10 % of lowest RMSE is defined as behavioral and B is defined as a subset of parameter values producing these behavioral results and
4. the calculations results in a number of distributions $f_j(X_i|B)$ that represent the contribution of parameter X_i to best possible fit of j -th observed series.

Plotting the distributions (or better the CDFs) is one step further to trace possible trade-offs. A trade-off is present, when at least two distributions differ from posterior distribution (denoted in Figures as `base`) and differ from each other.

⁷root mean square error

3.2 Results for LS model

(Ratto 2008a, p. 126) lists these parameters as the ones bearing biggest trade-offs: $\psi_1, \psi_3, \rho_R, \alpha, k, \rho_q, \rho_y^*$. This subsection compares and contrasts results obtained by (Ratto 2008a) and by this working paper.

In (Ratto 2008a), parameters ψ_1 and ψ_3 both represent similar trade-offs, albeit a bit smaller in volume in case of parameter ψ_3 . Both parameters should be rather smaller in order to fit inflation π and rather larger in order to fit the change in nominal exchange rate Δe . Realization of the LS model on Czech data tells a bit different story – see figure 9, panel one and three. ψ_1 and ψ_3 should be smaller in order to fit inflation optimally as in Ratto's realization on Canadian data, but the similarity with (Ratto 2008a) ends there. Both parameters fit the change in nominal exchange rate quite well in their posterior distribution; there will be no gain if they become bigger (unlike Ratto's result). Larger value of ψ_1 than its posterior distribution supports a better fit of output and interest rate. Results for ψ_3 are however somewhat different: interest rate supports a bit lower value, whereas output supports somewhat larger value. Figure 12 contains the same information, with the difference that PDFs are drawn instead of CDFs.

Indications of trade-offs associated with parameter ρ_R (ρ_R) are similar in Canadian and Czech realization of the LS model. Both realizations suggest that ρ_R should be lower in order to fit inflation better and higher in order to fit interest rate better. However, the magnitude is different. A deviation of the parameter from its posterior distribution is higher in the Czech model in case of interest rate and lower in case of inflation: see figure 9, panel 4.

Parameter α fits all variables rather well in both country realizations. Deviations are small and different in the two countries.

Parameter k is much more interesting. (Ratto 2008a) states that all observed series have a preference for a larger value of k . Posterior mode for k is somewhat less than .5 in (Ratto 2008a). The Czech model placed posterior mode of k to almost 2 and there is no longer a preference for bigger k from all variables. Inflation even prefers lower k than posterior distribution. Change in terms of trade Δq has a good fit at posterior distribution. Remaining three variables still prefer bigger value of k . For details see figure 10, panel 2.

Parameter ρ_q has also interesting trade-offs. Δq alone would imply a given value of the

parameter 0.5, which is almost at posterior mode. (Ratto 2008a) uses different calibration so that it encompasses different quantitative (but not qualitative) result of an estimate 0.26. Other variables in (Ratto 2008a) fit data rather well with ρ_q at posterior distribution. However, when we consider Czech data realization, it is no longer the case. Δe relatively strongly supports lower value of the parameter and inflation prefers somewhat higher value of the parameter, too.

No other parameter causes conflicts between fit of the variables and that holds for both Canadian and Czech data realization.

Figures 13, 14 and 15 depict CDFs for log-prior, log-likelihood and log-posterior. Sampling is done from prior ranges for all three figures. Red line stands for the density of the variable, that produces best 10 % RMSE. Green line then draws the remaining part of the sample and blue line represents the full sample. Since these pictures are not used in (Ratto 2008a), the interpretation is quite an open question.

The figures are drawn for observables, which are output growth y_{obs} , inflation πe_{obs} , interest rate R_{obs} , a change in the terms of trade dq and a change in the nominal exchange rate Δe . All figures have green and blue lines almost perfectly overlapping. This is a mere consequence of a fact that 90 % of samples is almost the same as the full sample (100 %).

Variable dq has all three lines overlapping in all three figures: It might mean that the groups producing best portion of RMSE and the rest are virtually the same values. All variables except dq in figure 13 demonstrate similar behavior: The red line is to the right from the remaining two, which suggests that the best 10 % RMSE are obtained by picking rather bigger values. However, looking at the other two figures 14 and 15, the picture becomes upside down. Variables dq , Δe and πe_{obs} seem not to have preference towards either bigger or smaller values. Remaining variables y_{obs} and R_{obs} seem to have opposite preference than in figure 13: The red line is to the left of the other two, which should indicate that the best 10 % RMSE are obtained with rather lower values. The issue with these "opposing preferences" might also be in values of the functions (and possibly used transformations). The documentation only mentions logarithmic transformation and there is a tenfold drop in values of the functions from log-prior to either log-likelihood or log-posterior. The values of the functions in figure 13 are from -300 to -100, whereas values of functions in figures 14 and 15 span from -3000 to -2000.

There are two more sets of similar pictures. Figure 16 shows similar results when sampling from multivariate normal. Finally, figure 17 shows similar results when using Metropolis posterior sample. Figure 16 displays no major differences among red, green and blue lines. Only log-likelihood and log-posterior values of y_{obs} and pie_{obs} seem to prefer slightly lower values. In other cases, the lines overlap. Again, there is a shift in values from log-prior to log-likelihood and log-posterior. Most values of log-priors are in the interval (0,10), whereas log-likelihood and log-posteriors span approximately from -530 to -495. Figure 17 is very similar to 16. The cdfs span on similar intervals and the same observed variables tend to lower values to reach best 10 % RMSE. There is just one noticeable difference, the best 10 % of RMSE are obtained by rather lower values (than the rest of the sample) for Δe for log-prior and log-posterior.

Table 5 displays bi-dimensional projections from prior sample of the best 10 % RMSE for cases, when correlation between two parameters exceeds 0.3 in absolute value. The columns of the table represent various observable variables, the rows represent varying sample size. Different sample sizes are depicted for a reason: Larger sample depicts the shape of the correlogram better and it is therefore easier to read the patterns. However, varied density of the points is more apparent in a correlogram computed on a smaller sample. The initial number of samples starts at 2,048, which is a default value. Then there are sample sizes of 4,096 and 20,480, which is 2 and 10 times larger than the original sample. Finally, there are two big sets of samples containing 50,000 and 100,000 samples. According to the results in table 3, some 97 % values of the subset correspond to behavioral set. Consequently, approximately 97 % of the samples pass the MCF procedure and are used to calculate the correlations. The exact numbers of samples used for calculation of the correlograms are 1,989; 3,976; 19,855; 48,475 and 96,955.

Column 1, 3 and 4 have varying number of figures. This dissension in the count is caused by a correlation coefficient being near the given threshold, |0.3|. At some sample size, the correlation coefficient is estimated to be somewhat larger (an the figure is thus drawn), at another sample size it may not be the case and the figure is not drawn since the correlation coefficient is in absolute value smaller than 0.3.

There are three different couples of parameters with significant correlation for observable variable π (inflation). These are ψ_1 vs. ψ_3 with a strong relationship, ψ_3 vs. ρ_{π^*} with a moderate relationship and finally ρ_{y^*} vs. α with a confusing relationship. Correlograms

for ψ_1 vs. ψ_3 depict negative correlation, which means that the sum of the two coefficients must have certain value in order to reach the best 10 % RMSE. The shape of the correlogram suggests, that the sum $\psi_1 + \psi_3$ should be rather lower, approximately in interval (1;5). Note the white triangle "0,1,1", an area corresponding to $\psi_1 + \psi_3 \leq 1$. This area produces non-behavior (indeterminacy) as was concluded from figure 5 earlier. Correlogram for ψ_3 vs. ρ_{π^*} is similar: Values of parameters should be rather smaller with an approximate rule $\frac{\psi_3}{2} + \frac{\rho_{\pi^*}}{0.7} < 1$. The last observed correlation is for ρ_{y^*} vs. α and it appeared only when calculating with the smallest sample of 2,048 original samples. Because the shape of the correlogram is also confusing, we may conclude that this results is an error stemming from a low number of samples or the correlation being in fact lower than 0.3 in absolute terms.

Interest rate R has also three couples of parameters that have to meet certain conditions in order to reach the best 10 % RMSE. All three couples display negative correlation and all occur no matter the sample size. The first correlogram (from left) is for ψ_3 vs. ρ_{π^*} . This couple occurred also for a fit of π and the correlogram looks almost the same. This means, that meeting the approximate rule $\frac{\psi_3}{2} + \frac{\rho_{\pi^*}}{0.7} < 1$ ensures to reach the best 10 % RMSE for π and R as well. Second correlogram is for ρ_R vs. k . This correlogram indicates that a better fit of R is obtained with rather larger values of the parameters with approximate rule $\frac{\rho_R}{0.8} + \frac{k}{3} > 1$. Last correlogram for ρ_A vs. ρ_{y^*} is quite weird. There seem to be three areas driven by different rules. One of them is along the line for $\rho_A = (0.75, 1)$ no matter the value of ρ_{y^*} . Second systematic part seem to be $\rho_A + \rho_{y^*} > 1$ and $\rho_{y^*} < 1$. This pattern becomes more apparent with (very) large number of samples. Last "almost systematic" part is somewhere along $\rho_A = 0.2$ but there are only a few points, which brings us to another point to make. In this case, the need for various sample sizes becomes apparent. There are three (almost?) systematic parts in correlograms for ρ_A vs. ρ_{y^*} , but the power of the systematic parts is very different. Correlograms for smaller sample size show that the first mentioned area along $\rho_A = (0.75, 1)$ is much more dense than area along $\rho_A = 0.2$, which is visible only in correlograms that used very high number of samples.

There are two different correlograms for output y . Both show positive correlation between parameters and both are bit hard to interpret. Correlation between k and τ occurs only in two (of five) sample sizes. It is probably on the borderline of 0.3. Correlograms for α vs. τ converge to correlation 0.5, which would (with the correlogram itself) indicate

a relationship of approximately $\frac{\alpha}{0.8} = \frac{\tau}{2.5}$. Such "rule" is very approximate and not very apparent in the correlogram (for any number of samples).

Last observable variable with significant correlations is a rate of change of nominal exchange rate Δe . Correlogram for α vs. ρ_{y^*} is clearly an error due to small sample. Remaining correlograms for α vs. ρ_q indicate that $\rho_q - 0.5 < \alpha$.

4 High dimensional model representation / Reduced form mapping

4.1 Theory

Consider a DSGE model written as

$$E_t\{g(y_{t+1}, y_t, y_{t-1}, u_t; \mathbf{X})\} = 0,$$

where y_t is a vector of endogenous variables, u_t is a vector of exogenous shocks and $\mathbf{X} = (X_1, \dots, X_k)$ is the array of structural parameters. Let Y be a generic output (there will be an example of what Y might actually be). A non-linear relationship

$$Y = f(X_1, \dots, X_k)$$

then holds. With the help of High Dimensional Model Representation (hereafter HDMR), this non-linear (unknown) relationship can be expressed as a finite decomposition of the function f :

$$f(X_1, \dots, X_k) = f_0 + \sum_i f_i + \sum_i \sum_{j>i} f_{ij} + \dots$$

The HDMR terms are

$$f_0 = E(Y)$$

$$f_i = E(Y|X_i) - f_0$$

$$f_{ij} = E(Y|X_i, X_j) - f(X_i) - f(X_j) - f_0$$

where $f_i \equiv f(X_i)$, $f_{ij} \equiv f(X_i, X_j)$ and so on. The f_i s are called the main effects and f_{ij} s are called the second order interaction effects and so on. The decomposition terms tell how much Y moves around its mean value f_0 as a relevant function. Notation of variance corresponds to $V(f_i) = V_i$ and $V(Y) = V$, the first order sensitivity index is $S_i = V_i/V$, second order $S_{ij} = V_{ij}/V$ and so on.

A scalar measure can be constructed to calculate relative importance of X_i on the variance of Y .

Exemplary application to DSGE model is as follows: Let the reduced form is

$$y_t = T y_{t-1} + B u_t$$

and the generic output Y will be entries in the transition matrix $T(X_1, \dots, X_k)$ or the matrix $B(X_1, \dots, X_k)$.

4.2 Results for LS model

Figure 18 depicts the usefulness of a $\log(-Y)$ transformation. Panels 1 and 3 depict histograms of the reduced form coefficient Y itself. The values are slightly negative and most of them are little less than zero. The histograms therefore form one very narrow spike skewed a little to negative values. Such shape seems inconvenient for further analysis, since there is little (if anything) we can see from such histograms.⁸ The $\log(-Y)$ transformation of the sample results in nicely shaped histograms as in Panel 2 and 4. Ratto's paper therefore uses this transformation throughout the HDMR analysis.⁹

Figures 19 and 20 depict first order HDMR for the two chosen reduced form coefficients. There are two variants for each of the coefficient: Y without transformation (left panels) and Y in transformation $\log(-Y)$ (right panels).

Figure 19 analyzes the influences that parameters of the model have on the reduced form structural coefficient $Y = (\pi_t \text{ vs. } R_{t-1})$, with and without logarithmic transformation. Solid lines that are inside dotted intervals mean that f_i term has zero value of and the corresponding parameter can have no influence on Y . Lines that cross the dotted lines represent f_i s that may have an influence on Y . The magnitude of the influence is judged by sensitivity index S_i . Index S_i expresses a fraction of variation of Y that is explained by i -th parameter.

Searching for non-zero S_i s in the left panel reveals that there are three of them. These are¹⁰ $S_{\rho_R} = .67$, $S_{\psi_1} = .04$, and $S_k = .01$, which totals to explanation of 72 % of

⁸There are other inconvenient results if we don't use any suitable transformation. Some of them are depicted in Figure 22.

⁹There are also other transformations, all of them are automated in Ratto's application and all of them lead to a nicely-shaped histogram.

¹⁰A compact notation shall be used: Sensitivity index S_i for parameter ψ_1 shall be S_{ψ_1} and so on...

total variance of Y . Right panel offers similar situation, yet somewhat different: $S_{\rho_R} = .89$, $S_{\psi_1} = .07$, $S_k = .02$ and $S_{\psi_3} = .01$, which sums to 99 % of total variance of $\log(-Y)$. The latter approach gives very similar results, but scores better. So it's another reason why to use the logarithmic transformation.

An analysis of the signs is conducted before passing to the next case. Basic questions are: What are the linkages between the two panels? What do the signs tell us in the right panel? By investigating statistically significant f_i s in both panels one observes that they change the sign of their slope. In another words, increasing f_i s in the left panel are decreasing in the right one and vice versa. This is due to the minus sign in the logarithmic transformation $\log(-Y)$. In right panel, larger values of ρ_R and k and smaller values of ψ_1 and ψ_3 imply larger values of $\log(-Y)$ transformation and therefore small (or – in another words – large negative) values of Y .

Figure 20 is constructed in the same way as figure 19 except it is calculated for reduced coefficient $Y = (\pi_t \text{ vs. } e_{R,t})$. Left panel has four parameters with nonzero sensitivity indices, these are $S_{\rho_R} = .64$, $S_{\psi_1} = .07$, $S_{\psi_3} = .01$ and $S_k = .01$. These parameters explain 73 % of variation of Y around its mean. Right panel presents the results for $\log(-Y)$ transformation with these nonzero sensitivity indices: $S_{\rho_R} = .66$, $S_{\psi_1} = .17$, $S_k = .07$, $S_{\psi_2} = .01$ and $S_{\psi_3} = .01$. Explanation of variation of $\log(-Y)$ is in this case 92 %.

To extract some information more easily, Ratto's G/LSA offers also graphs of ordering of sensitivity indices for each reduced form coefficient. Figure 21 displays the values of sensitivity indices as bars and sorts it from the highest to the lowest. This information is also present in figures 19 and 20, but this figuration is more suitable for detection of the most important parameters, especially when there are many reduced form coefficients to investigate. First two panels represent Y , second two panels represent $\log(-Y)$. Looking at the similarities of the two groups, we can yet again conclude that $\log(-Y)$ transformation doesn't bring in any unwanted effects.

Explanation capability of figure 22 isn't completely clear. There isn't any mention of it in the documentation of the G/LSA tool nor in the literature. The title of the graph says it is a fit of a reduced form coefficient. However, it doesn't say to what variable is the actual fit observed. Another question is¹¹, what is on the vertical axis. Histograms in figure 18 suggest that horizontal axis depicts the values of the reduced form coefficient.

¹¹It may be the same question as was suggested in the previous sentence.

Green points should probably form a regression line through the blue points.

Figure 23 depicts boxplots¹² of sensitivity indices. Right panels show results only for a given (small) set of relations. Left panels show results for all possible relations. This comparison is showed, because the right panels are default results of the analysis, although hardly interpretable. By choosing different variables, an analyst can change the picture almost arbitrarily. On the other hand, graphs calculated from all possible relations encompass all sensitivity indices and an analyst can therefore draw robust conclusions. Left panels again show that using $\log(-Y)$ transformation doesn't make much difference. Panel 1 is used for the interpretation of the results itself.

According to panel 1 of figure 23, the most influential parameters are ψ_1 , ρ_R , k and τ . The least influential parameters seem to be ψ_2 , rr and ρ_{y^*} . Parameter ψ_1 has highest median, but upper quartile and upper whisker isn't much higher. Such characteristics could mean that ψ_1 is important for many reduced form coefficients, but is rarely very important. Parameter ρ_R has highest upper quartile and upper whisker, but it has lower median than ψ_1 . This backward-looking parameter of the monetary rule is therefore quite important for many reduced form coefficients and very important for some, too. On the other hand, lower median would suggest that the number of reduced form coefficients for which is ρ_R important is lower than in the case of ψ_1 . Parameters k and τ are even less important than the two just discussed. Both have lower values of median and upper quartile. Upper whisker is somewhat lower, too.

Both parameters ψ_2 and rr have all sensitivity indices virtually zero, which should suggest that these parameters are unimportant for all possible reduced form coefficients. Boxplots of α , ρ_q , ρ_A , ρ_{y^*} and ρ_{π^*} represent rather peculiar results. All of these parameters have median and upper quartile virtually zero, but have some high outliers. Such results mean that these parameters are unimportant for most reduced form coefficients, but have important (in case of α) or very important (in case of the remaining four parameters) influence on some reduced form parameters.

¹²Extract from ([Matlab documentation](http://www.mathworks.com/access/helpdesk/help/toolbox/stats/boxplot.html)): `boxplot(X)` produces a box and whisker plot for each column of the matrix X. The box has lines at the lower quartile, median, and upper quartile values. Whiskers extend from each end of the box to the adjacent values in the data; by default, the most extreme values within 1.5 times the interquartile range from the ends of the box. Outliers are data with values beyond the ends of the whiskers. Outliers are displayed with a red + sign. (<http://www.mathworks.com/access/helpdesk/help/toolbox/stats/boxplot.html>)

5 Morris sampling / Screening

5.1 Theory

This subsection explains the concept of elementary effects for sensitivity analysis. Contents of this subsection is based on (Saltelli 2008, part 3.2–3.4, pages 110–121).

Elementary effect is defined as

$$EE_i = \frac{Y(X_1, X_2, \dots, X_{i-1}, X_i + \Delta, \dots, X_k) - Y(X_1, \dots, X_k)}{\Delta},$$

where Y is output, $X_i, i = 1, \dots, k$ are inputs. Δ is a value in $\left\{\frac{1}{p-1}, \dots, 1 - \frac{1}{p-1}\right\}$, where p is a number of selected levels that form the grid for sampling.

Various realizations of EE_i form a distribution F_i so that $EE_i \sim F_i$. A straightforward transformation can also be defined so that $|EE_i| \sim G_i$. Three important sensitivity indices can be computed from distributions F_i and G_i . These are $\mu_i = \frac{1}{r} \sum_{j=1}^r EE_i^j$, $\mu_i^* = \frac{1}{r} \sum_{j=1}^r |EE_i^j|$, and $\sigma_i^2 = \frac{1}{r-1} \sum_{j=1}^r (EE_i^j - \mu_i)^2$, where EE_i^j is an elementary effect relative to factor i computed along trajectory j and r is a number of selected trajectories¹³.

The theory about these three measures is that μ is an average elementary effect. The higher it is, the more important the parameter is. However, since the elementary effects can be positive and negative as well, the effects can cancel out while summing up to μ . Consequently, low value of μ_i doesn't mean that i -th parameter is unimportant. This lack of power is also a reason to construct alternative measure μ^* . This measure calculates with absolute values of elementary effects, so it doesn't matter if the elementary effects are positive or negative. Some extra information can be acquired by comparing μ and μ^* . Some combinations that may occur are the following:

- μ small, μ^* small: Easy case, the parameter in question is not influential.
- μ big positive, μ^* big positive: Also a clear case, the parameter is influential, elementary effects are positive.
- μ big negative, μ^* big positive: The parameter is influential, elementary effects are negative.

¹³This number is selected from a much larger set of trajectories M in a way that there is as high spread among them as possible. The sense in selecting r trajectories from the set M is that it dramatically reduces computation costs while the r trajectories may describe the whole set M quite well.

- μ small, μ^* big positive: Special case. The parameter is influential, elementary effects are positive and negative as well. The distribution F is probably not unimodal (with peaks in positive and negative domain). Since the elementary effects are far from one another, the measure σ will probably also be high. In this case, interpreting μ alone results in the so-called Type II error – failing to identify an influential factor.

Measure σ represents variation around μ and may also detect non-linear or some mutual relationship. High σ generally means that the parameter has quite different influences in different settings, which may indicate dependence on other parameters or other relationships altogether.

5.2 Results for LS model

Routines generating figure 24 needed some reprogramming. Panels 1–3 are flawed in some way and are depicted in order to easily visualize the reprogramming steps. Further analysis of results concentrates only on panels 4–6. Panel 4 depicts boxplots of σ_i , panel 5 depicts boxplots of μ_i and last panel 6 depicts boxplots of the most important measure of all three, μ_i^* . All distributions are normalized to 1 so that relative connections can be observed.

Last (sixth) panel of figure 24 depicts similar information as figure 23, with the difference in sampling mechanism. The former uses Morris sampling, the latter uses sampling from prior distributions. Strictly speaking, there is also a difference in what is actually displayed. Figure 24 depicts boxplots of measures based on elementary effects EE_i , whereas figure 23 depicts boxplots of sensitivity indices S_i . Nevertheless, these sensitivity measures are closely tied. The patterns are similar in both figures¹⁴, but the values of μ_i^* s are bigger than the values of sensitivity indices S_i . Except for bigger values, there are also other remarkable similarities and differences. The biggest difference may be observed for parameter α , which has sensitivity indices virtually zero (except for 5 outliers), but represent highest upper quartile for μ_i^* s. With the exception of parameter α , most important parameters in both figures are $\psi_1, \psi_3, \rho_R, k$ and τ . Very similar results in both figures 23 and 24 are for variables $rr, \rho_q, \rho_A, \rho_{y^*}$ and ρ_{π^*} .

The differences in figures 23 and 24 can be divided into two groups. One group displays an even overall shift in values, which is due to the different calculation of sensitivity measures.

¹⁴meaning panel 6 in figure 24 and panel 1 or 3 in figure 23

Another group displays uneven shifts in values, especially visible for parameter α . These disproportions can be probably attributed to a different sampling mechanism. To draw some final conclusion, results in panel 6 of figure 24 suggest that parameter ψ_2 is quite unimportant for any reduced form coefficient and rr is completely unimportant.

Panel 5 depicts boxplots of μ s. All parameters have elementary effects with both positive and negative signs. Two parameters tend to positive sign of elementary effects, these are ψ_3 and α . Parameter ψ_3 reaches negative values only with its whisker, whereas α has its lower whisker at -1. Panel 4 depicts boxplots of σ s. This panel looks very similar to panel 6 with μ^* s so that the higher the influence of the parameter, the higher the variance of the parameter. This observation is violated mainly by τ , which spans in panel 5 from -1 to 1. Such variance is maximal attainable, so it's the probable cause of its unusually high variance in panel 4. It is also worth mentioning that since most μ s are around zero, trying to interpret it without the use of μ^* s would probably lead to the Type II error explained above.

Parameters that are unimportant for any possible relation in the model may be hardly identifiable. Figure 25 is displayed in order to allow for an analysis of identifiability. Figure 24 suggests that parameter rr should be hardly identifiable and parameter ψ_2 may be hardly identifiable. Figure 25 reveals that both parameters rr and ψ_2 have prior and posterior distribution almost perfectly overlapping, which suggests that these parameters are either unidentifiable or were calibrated. The same overlapping of distributions is also visible for parameter k , but figure 24 shows that μ_k^* s are influential. Figure 23 shows in panel 1 and 3 that S_k s exceeds 0.5, which means that k explains 50 % of variability of at least some reduced form coefficient. These facts support a hypothesis that the observation of lack of identifiability made in figures 24 and 25 is not equivalent. The direction of the implications is rather from figure 24 to 25. In other words, the lack of identifiability observed in figure 25 doesn't mean that the parameter in question is unimportant for reduced form coefficients.

Figure 26 compares two different approaches to show what parameters are important for a given reduced form coefficient. First two groups of graphs was computed the same way as results in figure 21, but the results are for π vs. all lagged endogenous variables and all exogenous shocks. Second two groups of pictures are similar, but these are computed as a screening with Morris sampling. Again, as in comparison of figures 23 and 24, values calculated by Morris sampling are higher. However, there are some other differences that

cannot be attributed to this cause. Most of these differences are again driven by α as it has in the previous analysis. Parameter α is usually uninfluential in calculations from prior distributions, yet very influential when sampling with Morris method. This is the case for reduced form coefficients (π_t vs. y_{t-1}^*), (π_t vs. A_{t-1}), (π_t vs. $e_{y^*,t}$) and (π_t vs. $e_{A,t}$). Figure 26 offers another peculiar difference, which is visible in graphs for reduced form coefficients (π_t vs. y_{t-1}^*) and (π_t vs. $e_{y^*,t}$). Sampling from prior distributions results in just one important parameter τ , whereas sampling with Morris method results in 3–4 very important parameters (including τ and α).

Conclusion

This working paper investigated sensitivity properties of (Lubik and Schorfheide 2003) model, which is a small-scale structural general equilibrium model of a small open economy. The model is defined by equations (1)–(8). This case study uses quarterly Czech data from 1996 to 2008.

Stability mapping analysis results in a couple of useful outcomes. Preferable type of sampling seems to be from multivariate normal and the size of the sample doesn't have to be very large. Results for LS model show that there is only one concern for stability and that is the so-called generalized Taylor principle $\psi_1 + \psi_3 > 1$. If this formula doesn't hold, Blanchard Kahn condition is violated and the solution of the rational expectations model couldn't be found.

Mapping the fit led to several interesting results. For some parameters (like k), this working paper's calibration of the model seems to have more favorable results, because there are less trade-offs for fit. For some other parameters (like ρ_q), results of (Ratto 2008a) seem to be better. Bi-dimensional projections of couples of parameters for attaining the best 10 % RMSE offers a different point of view on the characteristics of the best possible fit of trajectories of observable variables. Except for finding several relations that should hold in order to reach the best 10 % RMSE, this part of analysis also shows the importance of using several sample sizes, from the smallest to the largest.

Reduced form mapping elaborates influences of parameters to connections of two variables (or – in another words – reduced form coefficients). Subsection 4.2 also makes a successful search for most influential parameters (which are ψ_1, ρ_R, k and τ) and least influential

parameters (which are ψ_2 , rr and ρ_{y^*}).

Results about the (non)influence of parameters are compared to Morris sampling results. Outputs of these two approaches seem to be compatible. Final part of section 5 deals with the ability to identify parameters. One of the conclusions is that parameters rr and ψ_2 are either unidentifiable or were calibrated.

This working paper made a thorough sensitivity analysis of (Lubik and Schorfheide 2003) model with M. Ratto's G/LSA tool. This study is much more complex than the original article (Ratto 2008a), it explains some aspects of G/LSA in greater detail and it shows much more results than (Ratto 2008a) did. Since this work set a benchmark, the next logical step of research is to study different models and/or different economies.

References

- (Dynare) JUILLARD, Michel *et al.*: Dynare software package.
Homepage:
<http://www.cepremap.cnrs.fr/dynare/>
- (Griffoli 2007) GRIFFOLI, Tommaso Mancini: Dynare v4 – User guide,
Available online at
http://www.cepremap.cnrs.fr/juillard/mambo/download/manual/Dynare_UserGuide_WebBeta.pdf,
2007, cited draft: March 2007.
- (Lubik and Schorfheide 2003) LUBIK, Thomas, SCHORFHEIDE, Frank: Do Central Banks Respond to Exchange Rate Movements? A Structural Investigation, in *Economics Working Paper Archive*, n. 505, The Johns Hopkins University, Department of Economics, 2003
- (Matlab documentation) Matlab documentation: Available online:
<http://www.mathworks.com/access/helpdesk/help/>

[helpdesk.html](#)

- (Ratto 2008a) RATTO, Marco: Analysing DSGE Models with Global Sensitivity Analysis, in *Computational Economics*, Volume 31, Number 2 / March, 2008, pp 115-139, ISSN 0927-7099 (Print) 1572-9974 (Online)
- (Ratto 2008b) RATTO, Marco: Sensitivity Analysis Toolbox for DYNARE. Available online at http://eemc.jrc.ec.europa.eu/EEMCArchive/Software/DynareCourse/GSA_manual.pdf, version: April 18, 2008.
- (Saltelli 2004) SALTELLI, Andrea *et al.*: Sensitivity Analysis in Practice: A Guide to Assessing Scientific Models, John Wiley & Sons, Ltd., 2004, ISBN 0-470-87093-1
- (Saltelli 2008) SALTELLI, Andrea *et al.*: Global sensitivity analysis. The Primer. John Wiley & Sons, Ltd., 2008, ISBN 978-0-470-05997-5

A Tables

WP n.	M n.	Description	Note/Group
y	y	real aggregate output	
π	pie	CPI inflation rate	
R	R	nominal interest rate	
q	—	terms of trade ¹⁵	
Δq	dq	change in terms of trade	observable variable
y^*	y_s	exogenous world output	
π^*	pie_s	world inflation shock	
e	—	nominal exchange rate	
Δe	de	change in nominal exchange rate	observable variable
z	A	growth rate of the world technology progress	
\bar{y}	—	potential output	$\bar{y}_t = -\alpha(2 - \alpha)^{\frac{1-\tau}{\tau}} y_t^*$
y_{obs}	y_obs	growth of real output	$y_{obs,t} = y_t - y_{t-1} + z_t$, observable variable
R_{obs}	R_obs	annualized nominal interest rate	$R_{obs} = 4R$, observable variable
π_{obs}	pie_obs	annualized inflation	$\pi_{obs} = 4\pi$ observable variable
α	$alpha$	import share	$0 < \alpha < 1$
τ	tau	inverse elasticity of intertemporal substitution ¹⁶	$\frac{1}{\tau} > 0$
k	k	composite parameter	
β	—	(subjective) discount factor	$\beta = e^{-\frac{rr}{400}}$
rr	rr	steady state real interest rate	$rr = -400 \cdot \log(\beta)$
ρ_R	rho_R	interest rate smoothing term	$0 < \rho_R < 1$
ψ_1	$psi1$	policy coefficient	$\psi_1 > 0$
ψ_2	$psi2$	policy coefficient	$\psi_2 > 0$
ψ_3	$psi3$	policy coefficient	$\psi_3 > 0$
ρ_q	rho_q	AR1 coefficient	
ρ_{y^*}	rho_ys	AR1 coefficient	
ρ_{π^*}	rho_pies	AR1 coefficient	
ρ_z	rho_A	AR1 coefficient	

Table 1: Description of variables and parameters. WP n. = working paper notation, M n. = Matlab notation

¹⁵defined as the relative price of exports in terms of imports

¹⁶ $\frac{1}{\tau}$ is the elasticity of substitution

Time series	Symbol
Growth of real GDP per working person (demeaned)	y_obs
Inflation (annualized, demeaned)	pie_obs
Nominal p. a. interest rate (demeaned)	R_obs
Exchange rate change (demeaned)	de
Terms of trade change (demeaned)	dq

Table 2: Data set and its denotation

Priors	Size of sample	Stable share	Indeterminacy share
Uniform priors	2,048	97.1 %	2.88 %
Uniform priors	10,000	96.9 %	3.06 %
Prior distributions	10,000	95.1 %	4.9 %

Table 3: Summary results of stability mapping for different samples

Parameter	Uniform prior 2,048 samples		Uniform prior 10,000 samples		Prior distributions 10,000 samples	
	<i>d</i>	<i>p</i> -value	<i>d</i>	<i>p</i> -value	<i>d</i>	<i>p</i> -value
ψ_1	0.9120	2.62e-043	0.9020	2.36e-213	0.9320	0
ψ_2	0.0486	0.999	0.0192	1	0.0128	1
ψ_3	0.6220	2.37e-020	0.6130	1.35e-098	0.2780	5.58e-032
ρ_R	0.0312	1	0.0159	1	0.0141	1
α	0.0537	0.995	0.0159	1	0.0150	1
rr	0.0782	0.861	0.0237	0.996	0.0194	0.994
k	0.0821	0.818	0.0275	0.977	0.0166	0.999
τ	0.0872	0.757	0.0498	0.443	0.0246	0.938
ρ_q	0.0971	0.631	0.0291	0.961	0.0127	1
ρ_A	0.0412	1	0.0160	1	0.0152	1
ρ_{y^*}	0.0629	0.973	0.0215	0.999	0.0168	0.999
ρ_{π^*}	0.0565	0.991	0.0182	1	0.0105	1

Table 4: Detailed results of stability mapping for different samples

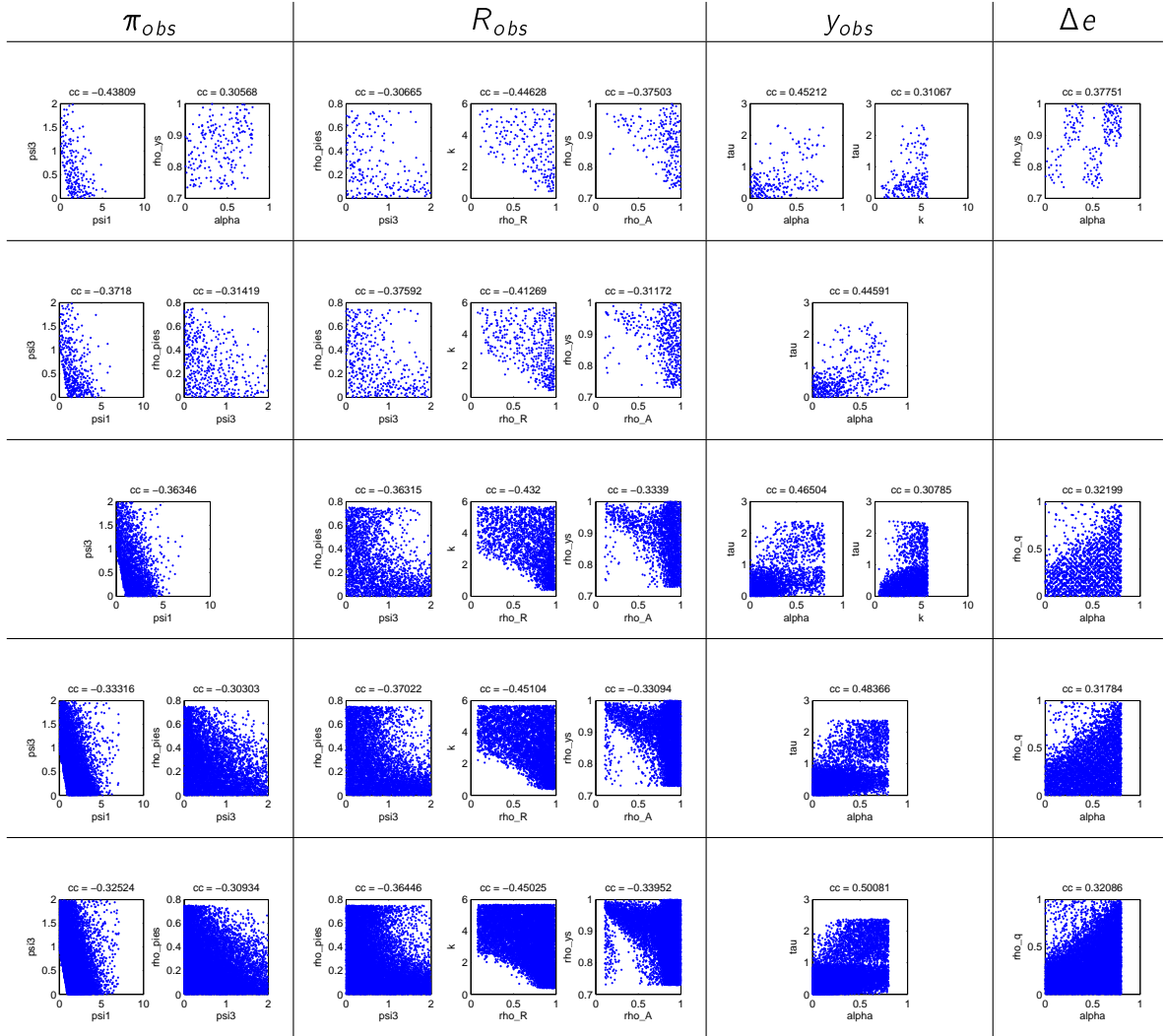


Table 5: Bi-dimensional projection for best 10 % RMSE. Prior sample. Sampled uniformly from prior ranges. The size of the sample is approximately 2, 4, 20, 50, and 100 thousands, respectively.

B Figures

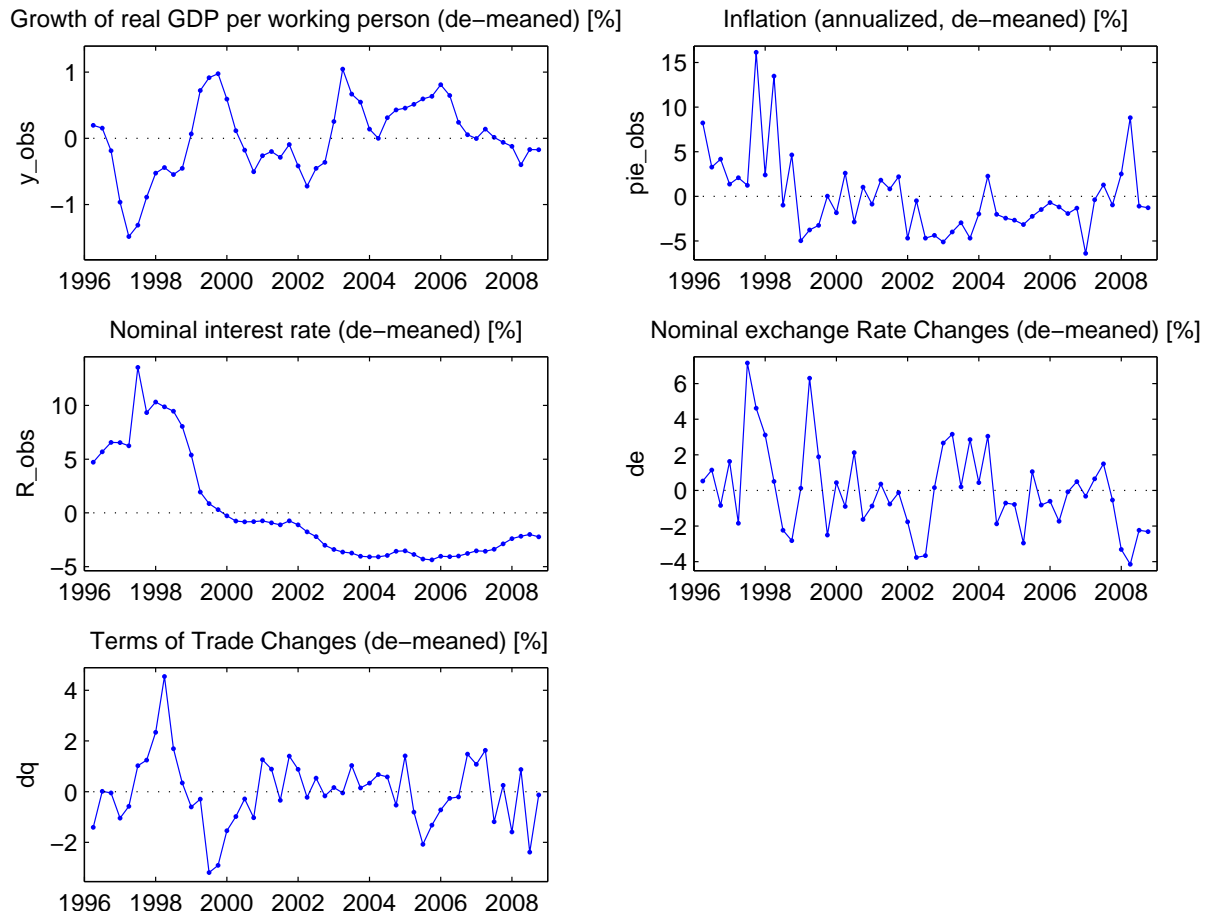


Figure 1: The data (observable variables). Time notation: 1996.25 is the first quarter of 1996 and 1997.00 is the last quarter of 1996.

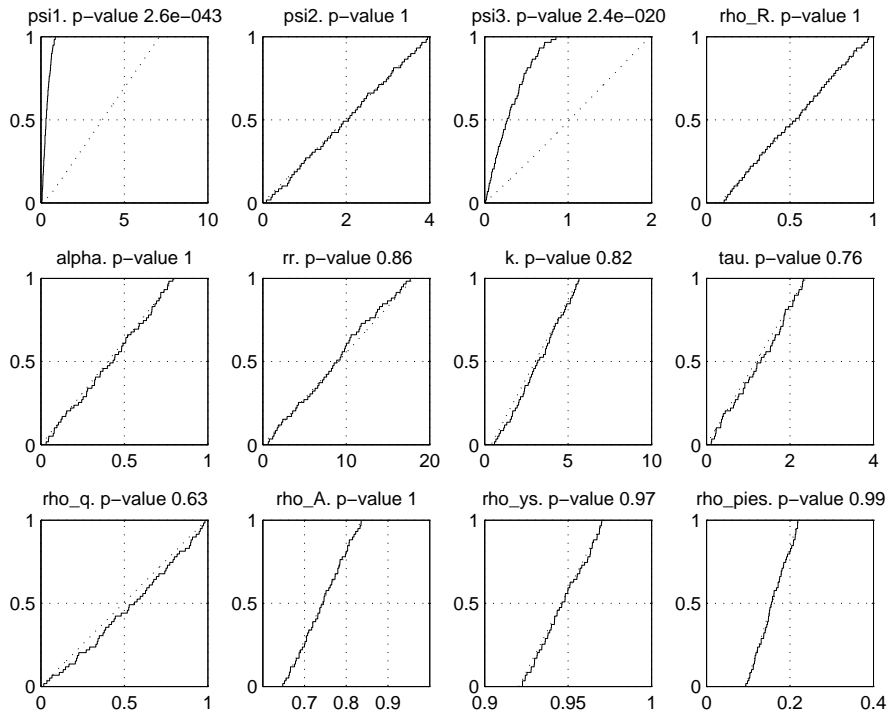


Figure 2: Smirnov test for stability analysis. Sample drawn uniformly from prior ranges, 2,048 samples. Solid lines are CDFs for non-behavior set $F_{\bar{n}}(X_i|\bar{B})$, dotted lines are CDFs for behavior set $F_n(X_i|B)$.

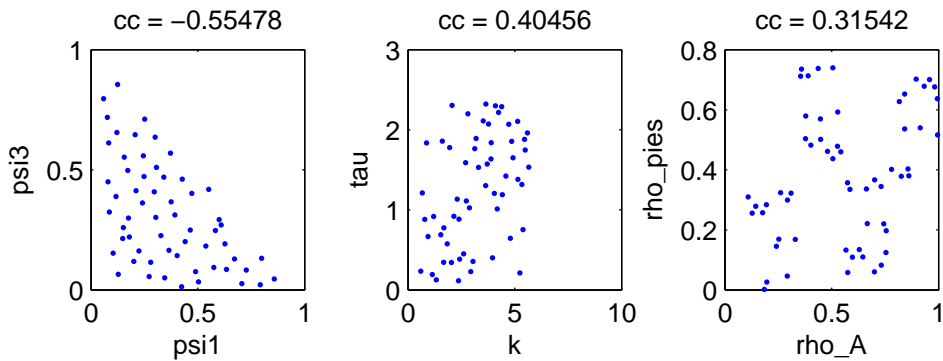


Figure 3: Bi-dimensional projection of parameters driving unacceptable behavior. Sample drawn uniformly from prior ranges, 2,048 samples.

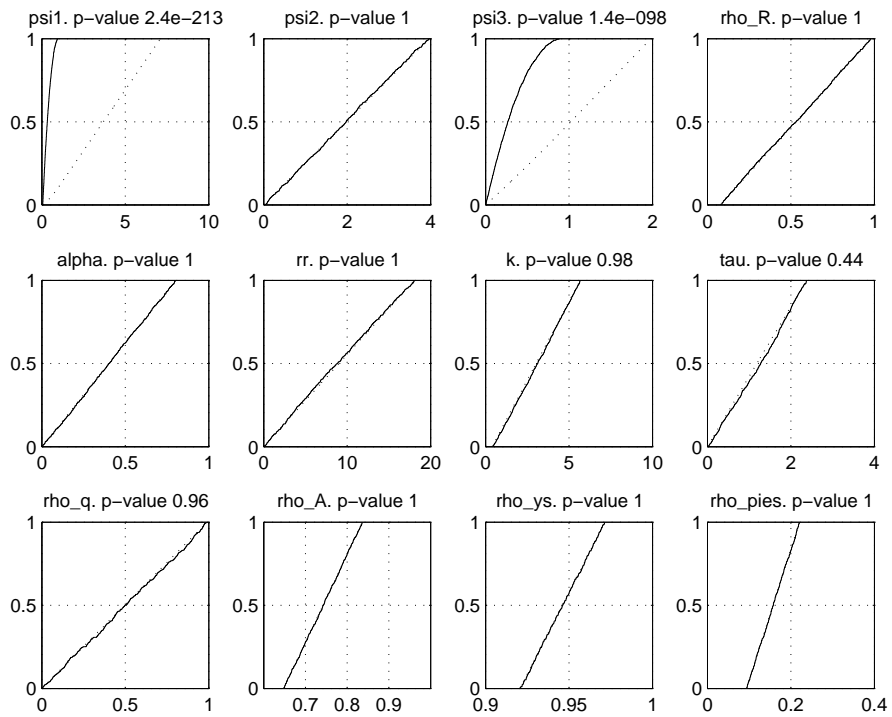


Figure 4: Smirnov test for stability analysis. Sample drawn uniformly from prior ranges, 10,000 samples. Solid lines are CDFs for non-behavior set $F_{\bar{n}}(X_i|\bar{B})$, dotted lines are CDFs for behavior set $F_n(X_i|B)$.

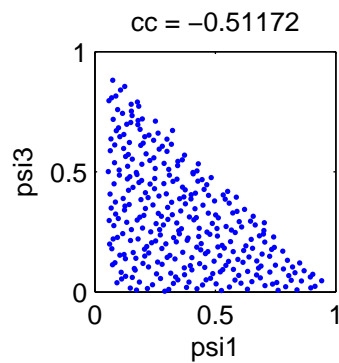


Figure 5: Bi-dimensional projection of parameters driving unacceptable behavior. Sample drawn uniformly from prior ranges, 10,000 samples

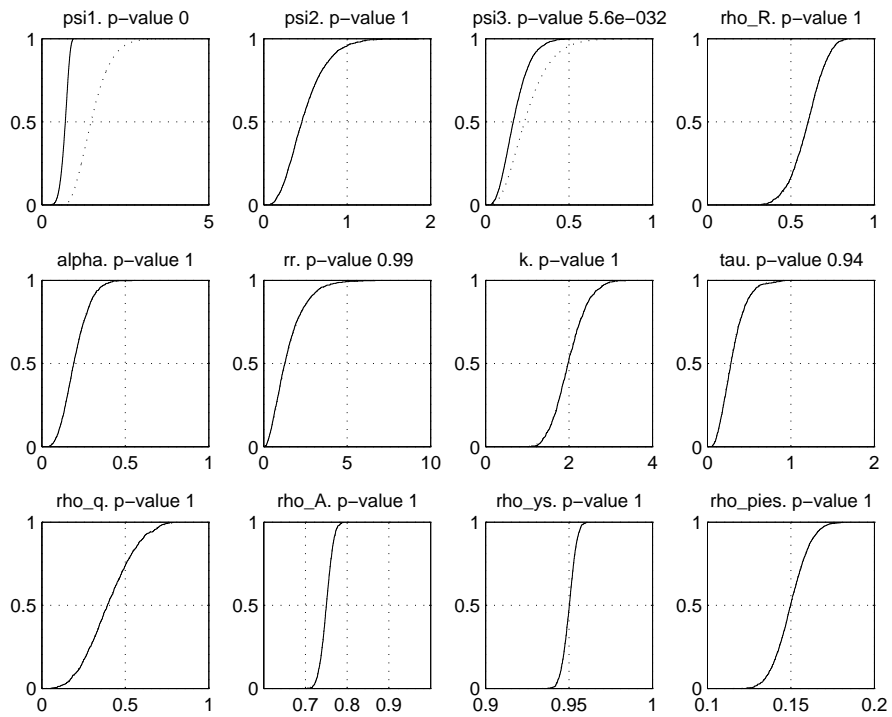


Figure 6: Smirnov test for stability analysis. Sample drawn from prior distributions, 10,000 samples. Solid lines are CDFs for non-behavior set $F_n(X_i|\bar{B})$, dotted lines are CDFs for behavior set $F_n(X_i|B)$.

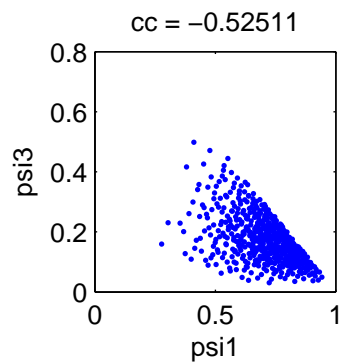


Figure 7: Bi-dimensional projection of parameters driving unacceptable behavior. Sample drawn from prior distributions, 10,000 samples.

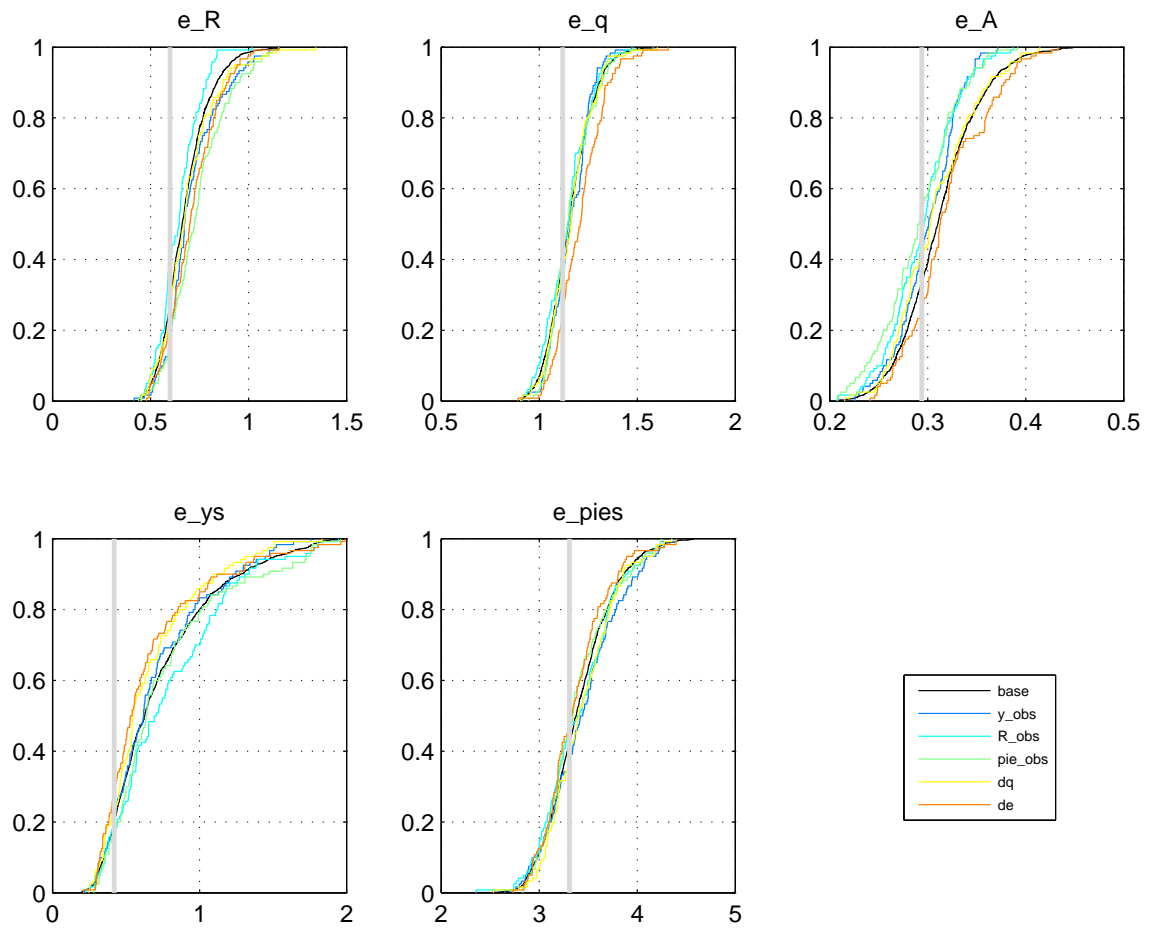


Figure 8: Cumulative posterior distributions (base) and the distributions of the filtered samples corresponding to the best fit for each singular observed series. Grey vertical lines denote posterior mode. (1 of 4)

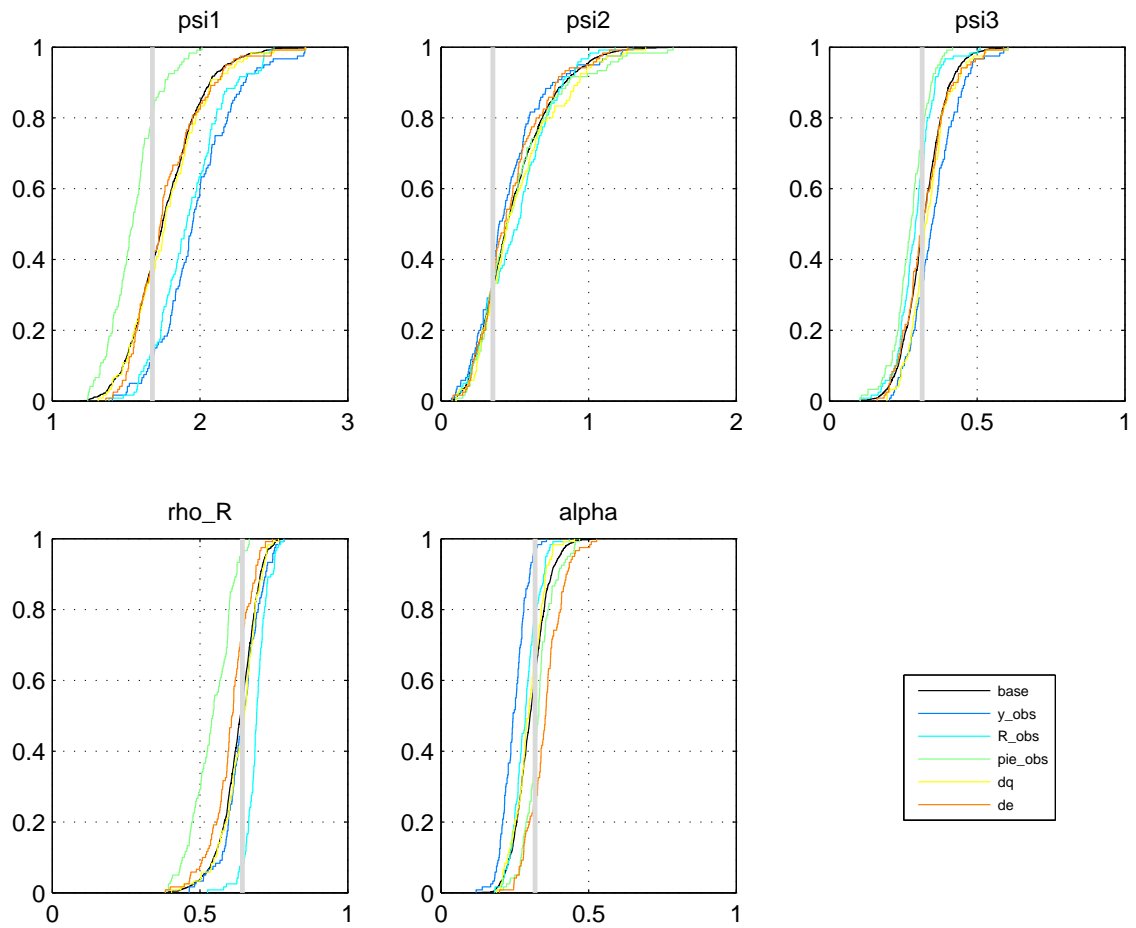


Figure 9: Cumulative posterior distributions (base) and the distributions of the filtered samples corresponding to the best fit for each singular observed series. Grey vertical lines denote posterior mode. (2 of 4)

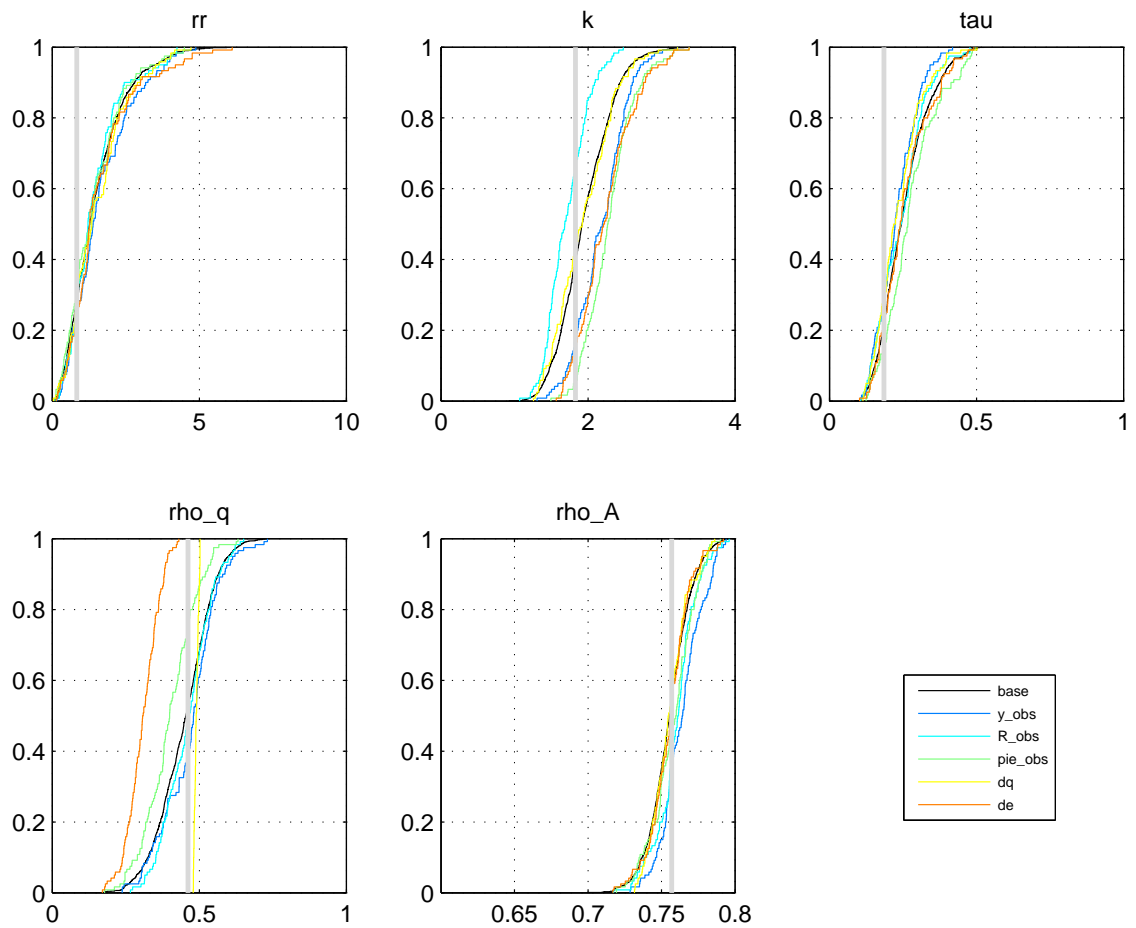


Figure 10: Cumulative posterior distributions (base) and the distributions of the filtered samples corresponding to the best fit for each singular observed series. Grey vertical lines denote posterior mode. (3 of 4)

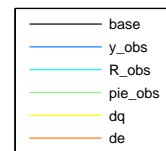
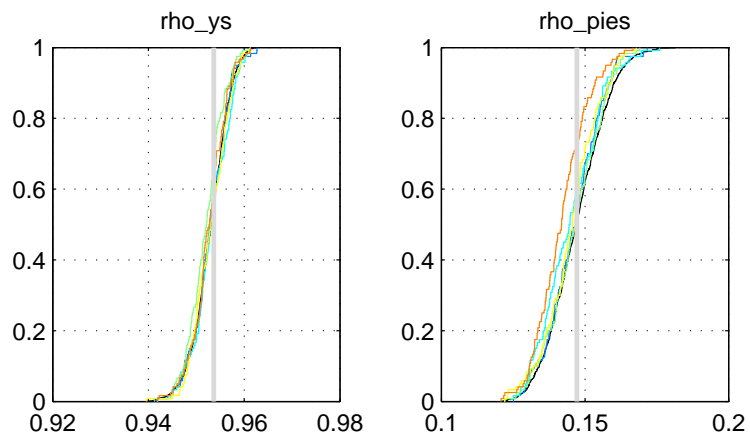


Figure 11: Cumulative posterior distributions (base) and the distributions of the filtered samples corresponding to the best fit for each singular observed series. Grey vertical lines denote posterior mode. (4 of 4)

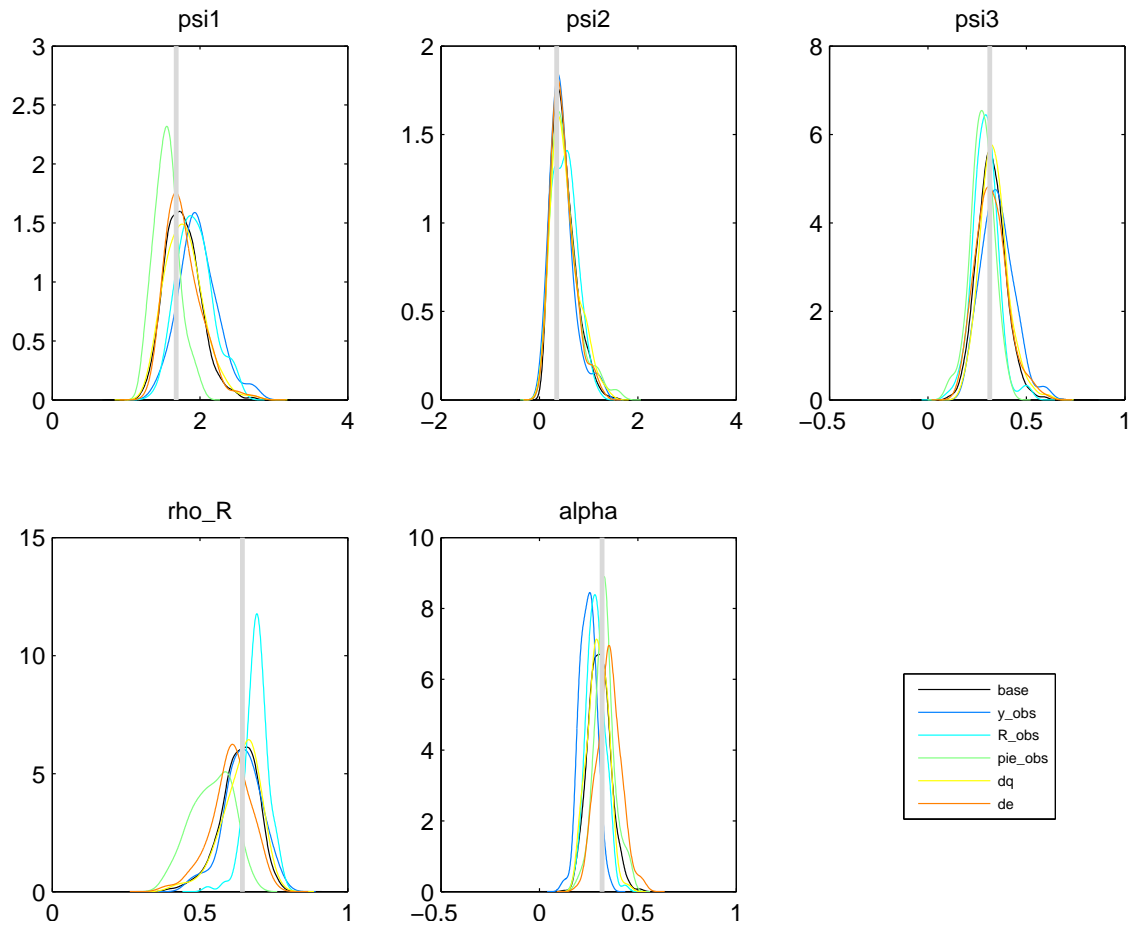


Figure 12: Posterior distributions (base) and the distributions of the filtered samples corresponding to the best fit for each singular observed series. Grey vertical lines denote posterior mode. Corresponds to Figure 9

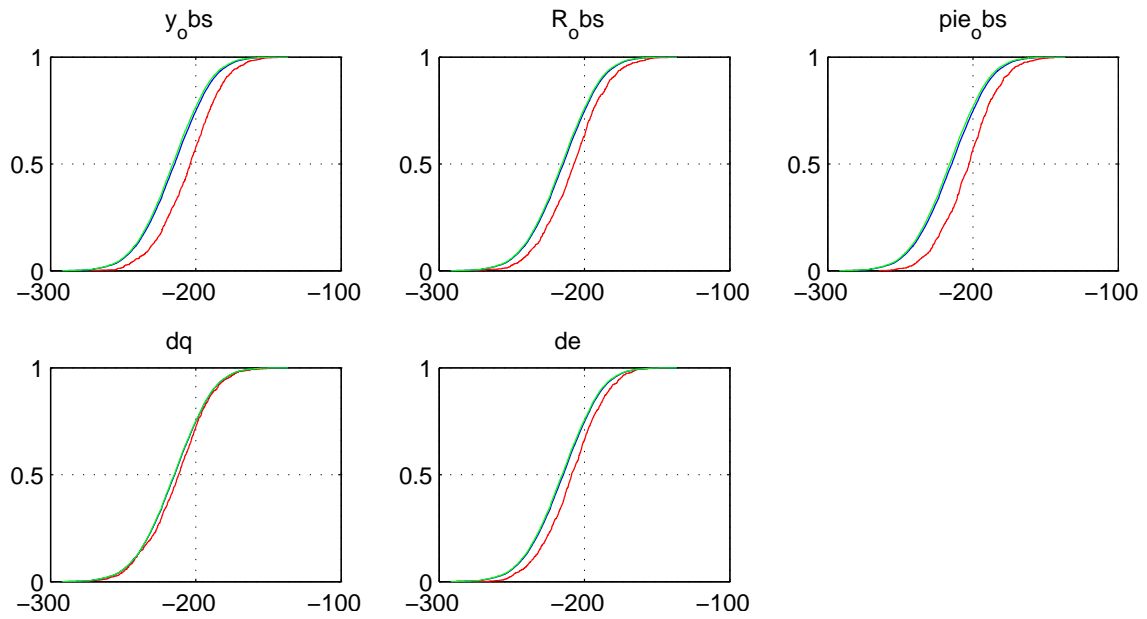


Figure 13: CDFs of the log-prior: red: best 10 % RMSE, green: rest of the sample, blue: full sample. Sampling from prior ranges.

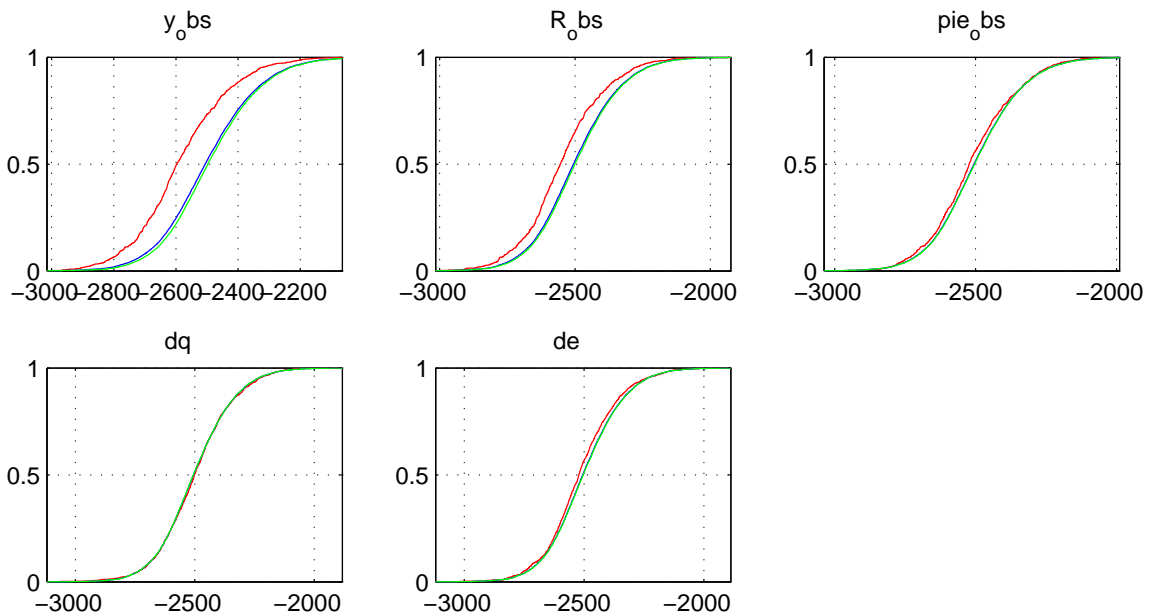


Figure 14: CDFs of the log-likelihood: red: best 10 % RMSE, green: rest of the sample, blue: full sample. Sampling from prior ranges.

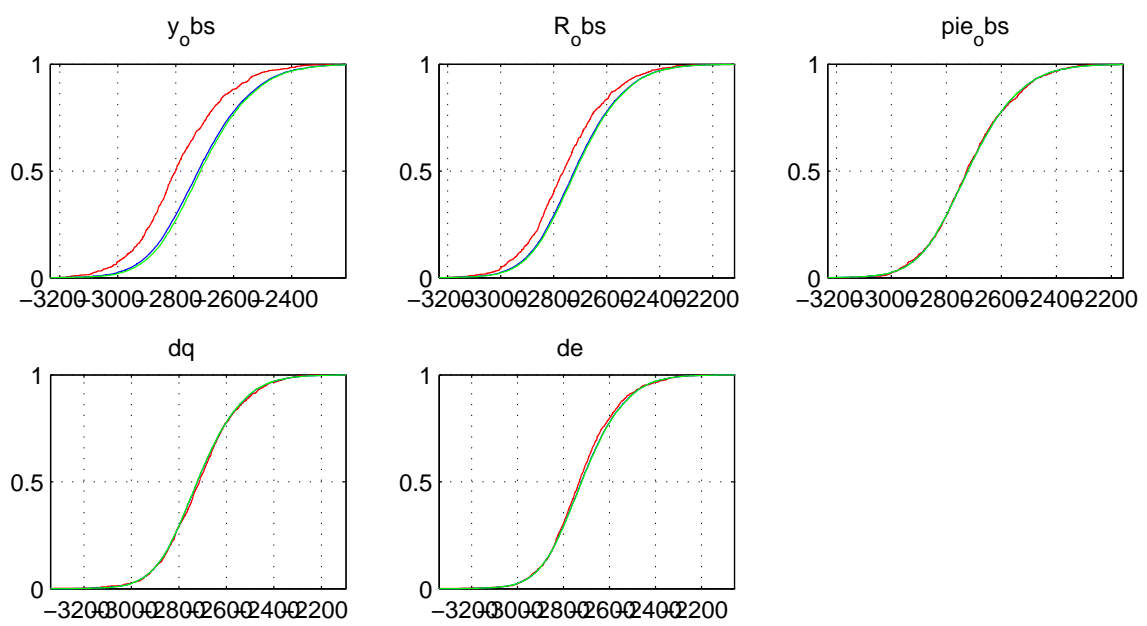


Figure 15: CDFs of the log-posterior: red: best 10 % RMSE, green: rest of the sample, blue: full sample. Sampling from prior ranges.

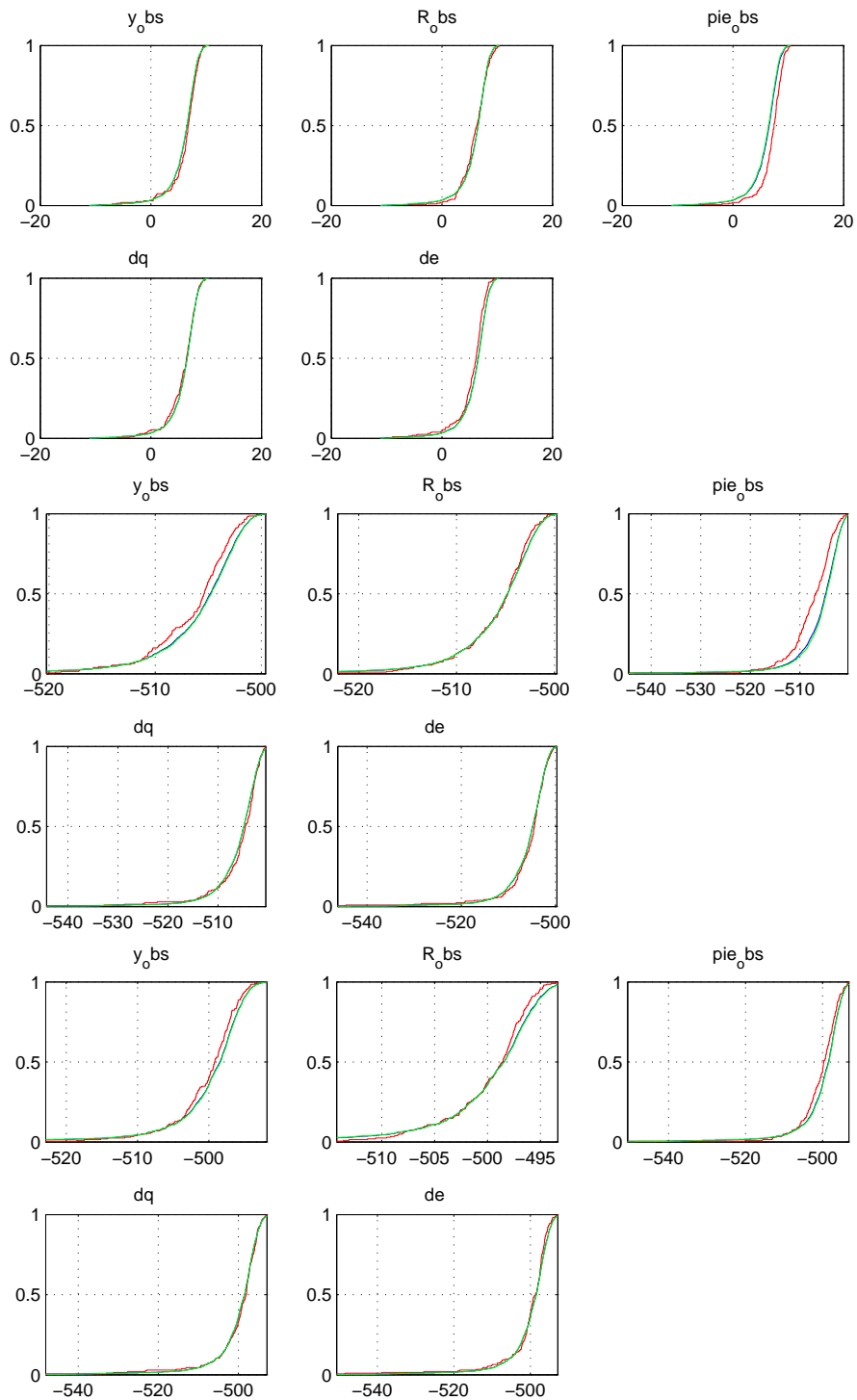


Figure 16: CDFs of the log-prior, log-likelihood and log-posterior: red: best 10 % RMSE, green: rest of the sample, blue: full sample. Sampling from multivariate normal.

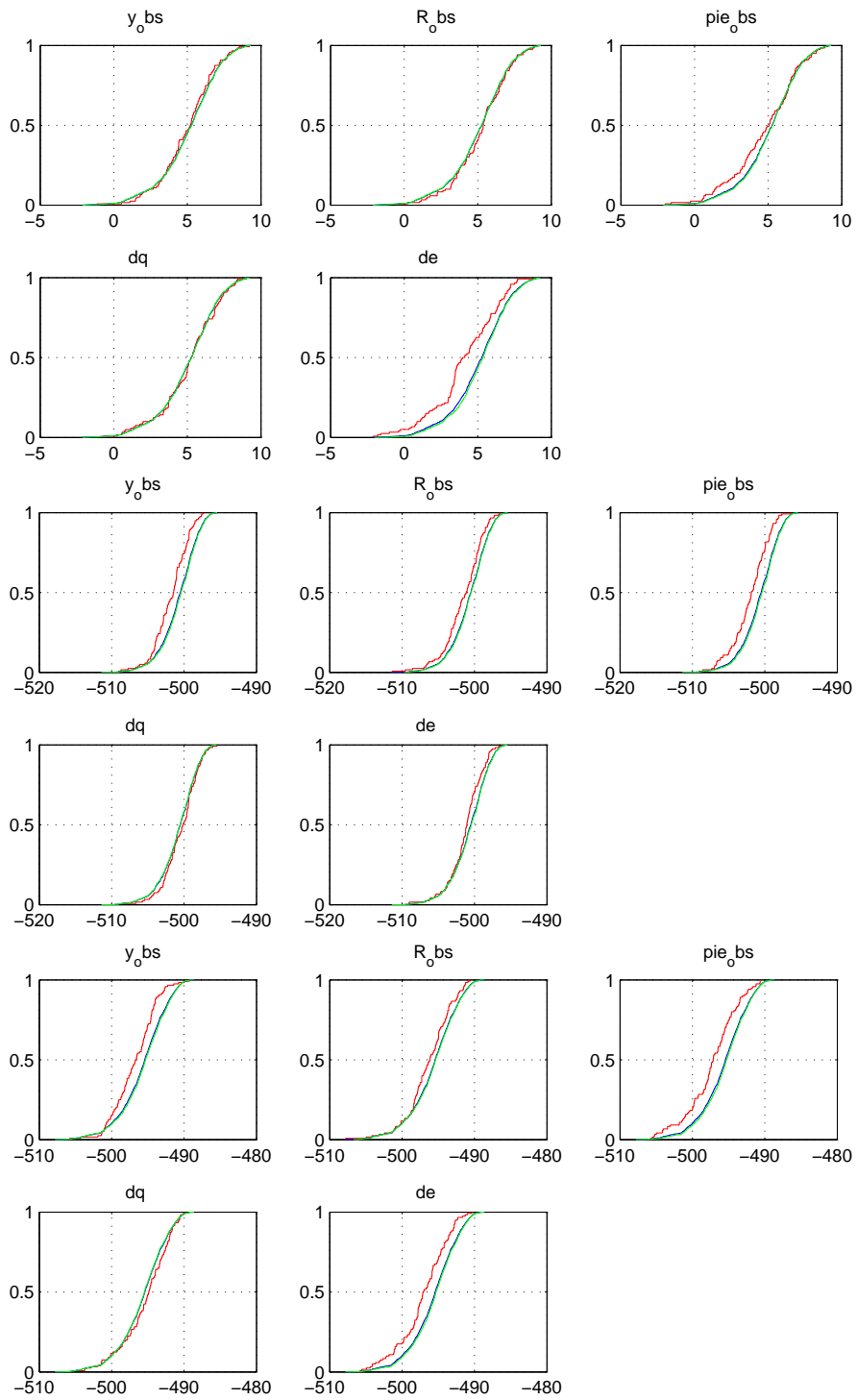


Figure 17: CDFs of the log-prior, log-likelihood and log-posterior: red: best 10 % RMSE, green: rest of the sample, blue: full sample. Using Metropolis posterior sample.

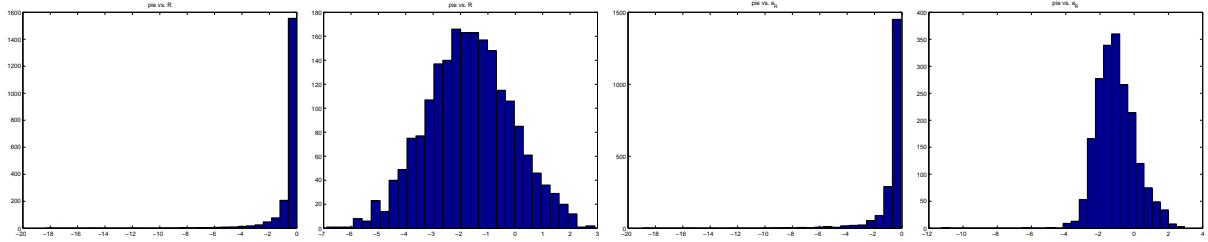


Figure 18: Histograms of the MC sample of the reduced form coefficient $Y = (\pi_t \text{ vs. } R_{t-1})$ (Panel 1–2) and $Y = (\pi_t \text{ vs. } e_{R,t})$ (Panel 3–4). Panels 1 and 3: actual values Y ; panels 2 and 4: $\log(-Y)$. Ratto's Figs. 12 and 13

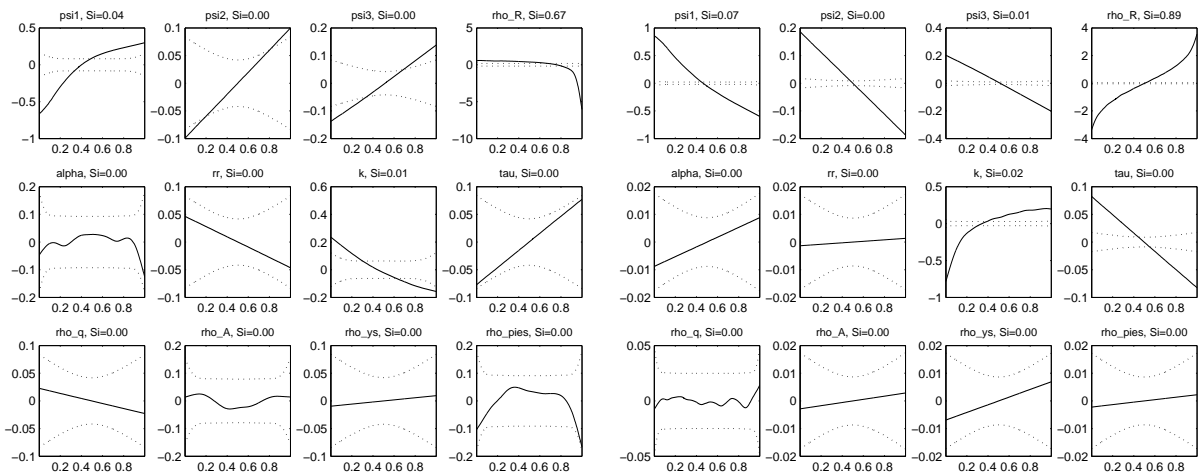


Figure 19: HDMR of the reduced form coefficient $Y = (\pi_t \text{ vs. } R_{t-1})$ in the $\log(-Y)$ transformation (right panel) and without transformation (left panel). Solid line: f_i terms, dotted line: 99.9% confidence bounds. $S_i = V(f_i)/V(Y)$ is a sensitivity index. Right panel is Ratto's Fig. 14.

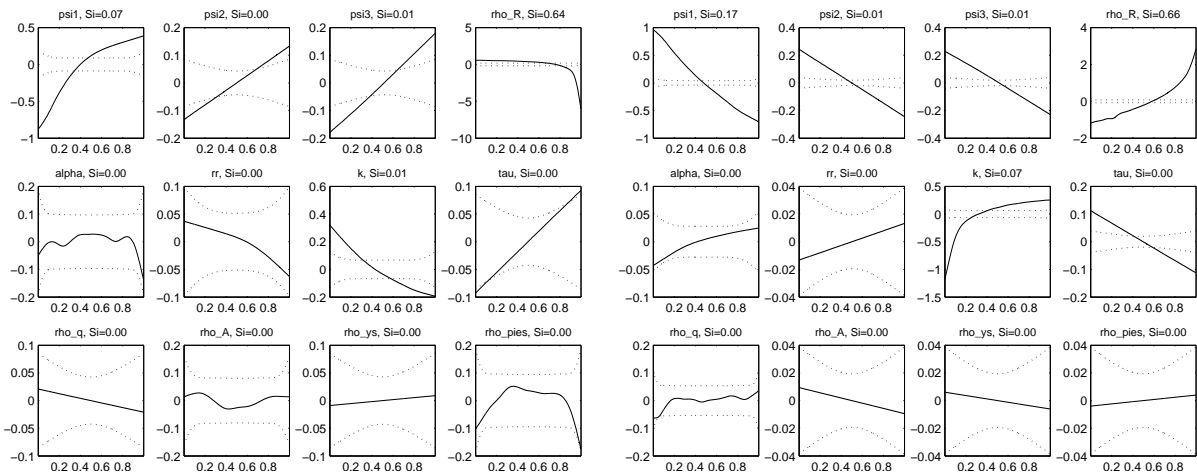


Figure 20: HDMR of the reduced form coefficient $Y = (\pi_t \text{ vs. } e_{R,t})$ in the $\log(-Y)$ transformation (right panel) and without transformation (left panel). Solid line: f_i terms, dotted line: 99.9% confidence bounds. $S_i = V(f_i)/V(Y)$ is a sensitivity index. Right panel is Ratto's Fig. 15.

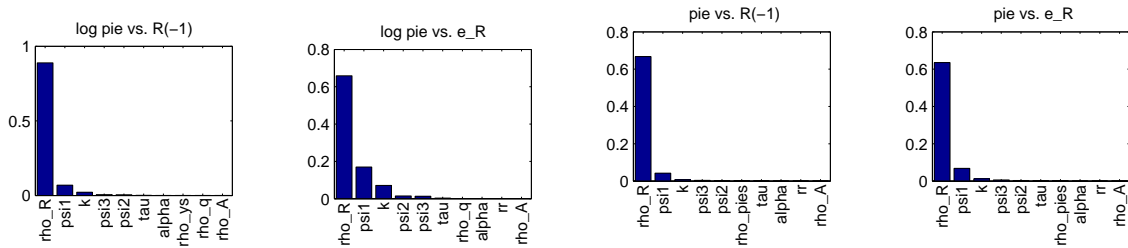


Figure 21: Ordering of sensitivity indices. Computation of $\pi_t \text{ vs. } R_{t-1}$ and $e_{R,t}$. First two panels show results with utilizing the $\log(-Y)$ transformation, third and fourth panels show results without transformation.

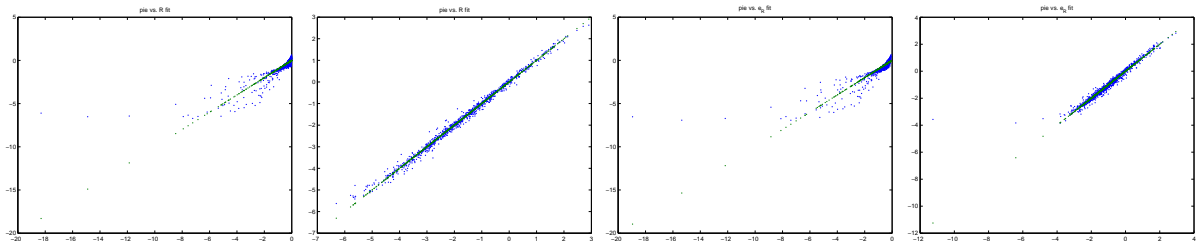


Figure 22: Fit of the reduced form coefficient $Y = (\pi_t \text{ vs. } R_{t-1})$ (panel 1 and 2) and $Y = (\pi_t \text{ vs. } e_{R,t})$ (panel 2 and 3) with (panel 2 and 4) and without (panel 1 and 3) $\log(-Y)$ transformation.

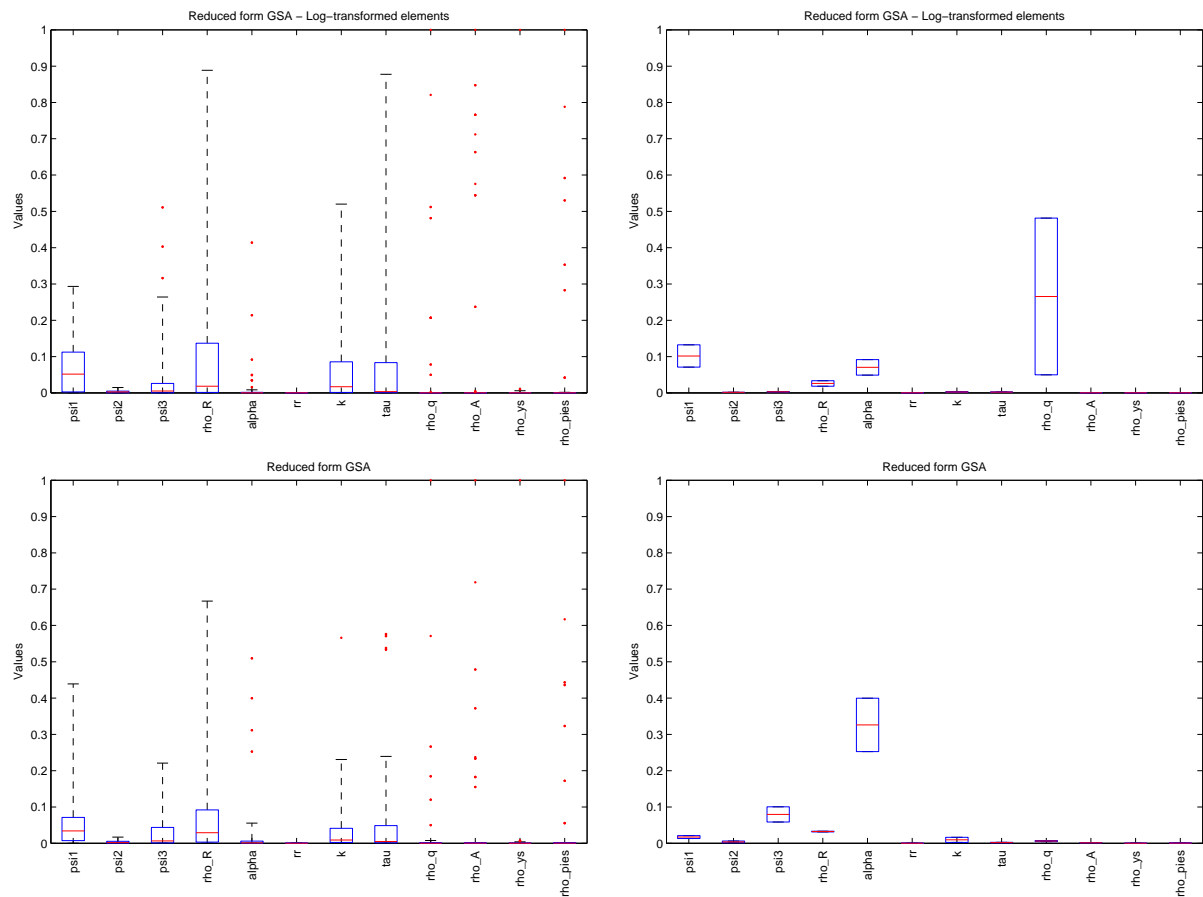


Figure 23: Boxplots of sensitivity indices. Left panels: All endogenous variables vs. all exogenous and all lagged endogenous. Right panels: π_t vs. $e_{q,t}$ and vs. Δq_{t-1} . First row of panels is with $\log(-Y)$ transformation and second row is without a transformation.

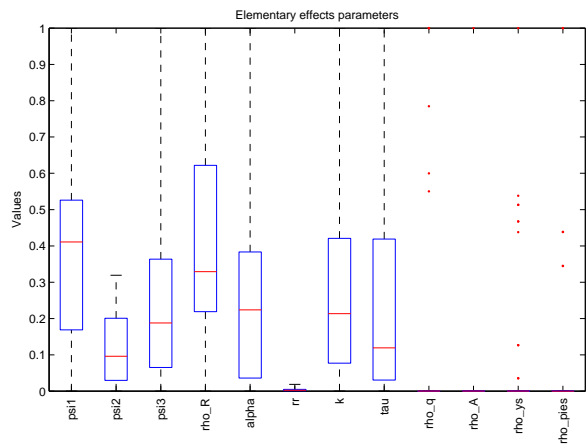
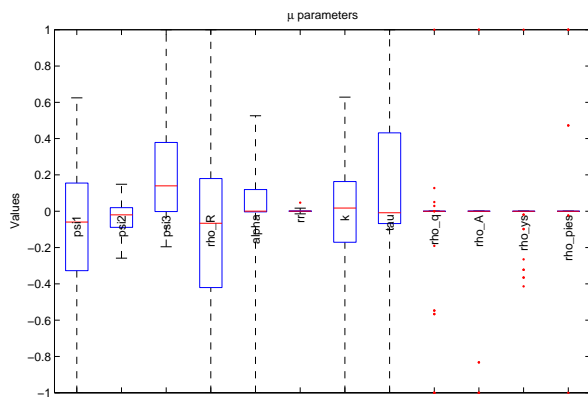
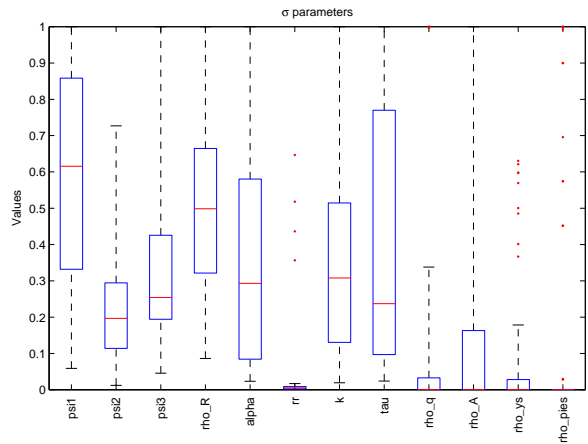
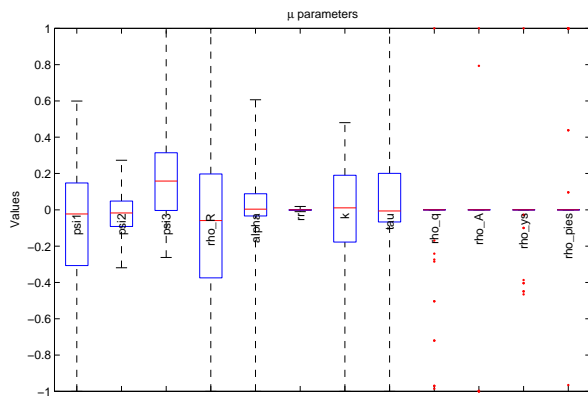
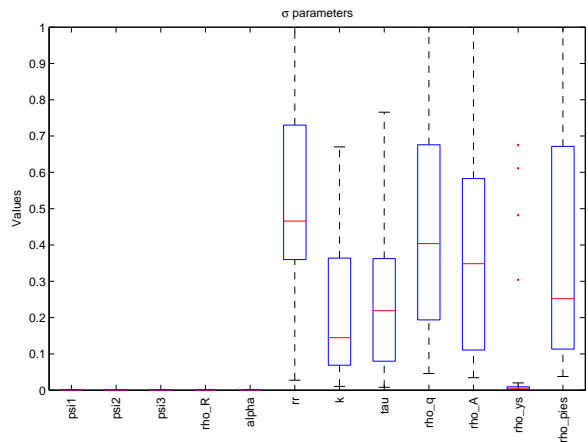
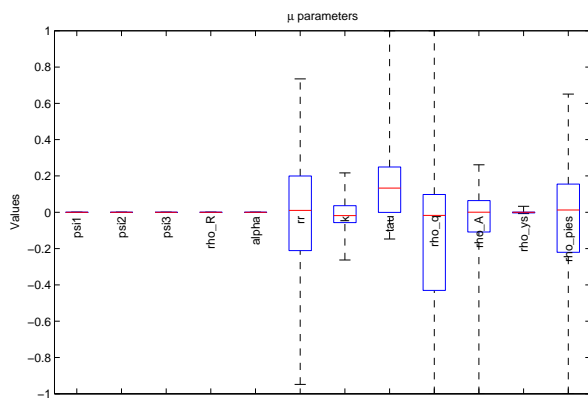


Figure 24: μ_i and σ_i boxplots computed from distribution F_i where $EE_i \sim F_i$. Morris sampling. First two panels computed by original G/LSA application. Second two panels are a result of a re-programming by Jan Čapek. Panel 5 is once again re-programmed to normalize to $\max |\mu_i|$. Panel 6 is μ_i^* originally computed by G/LSA.

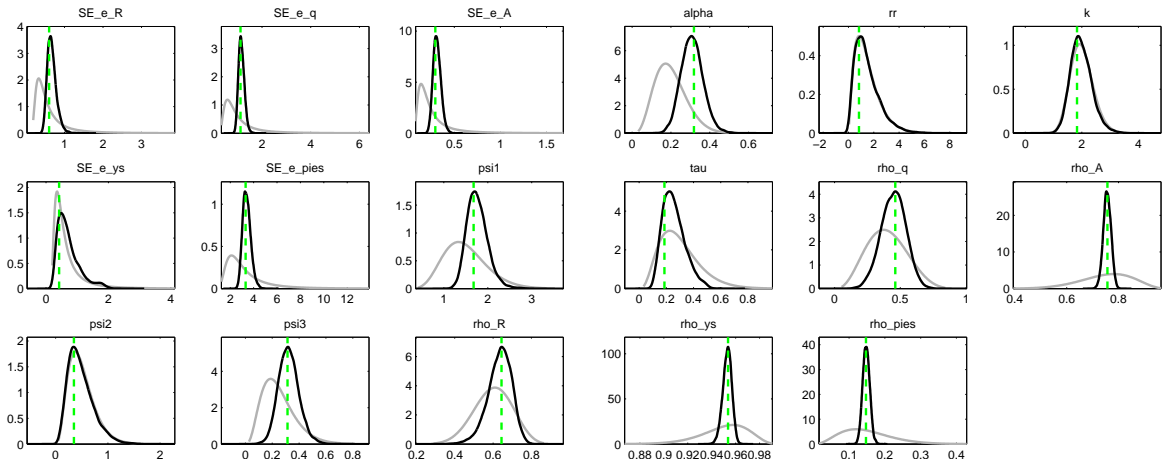


Figure 25: Prior (grey lines) and posterior (black lines) distributions of the parameters with posterior mode (green dashed lines).

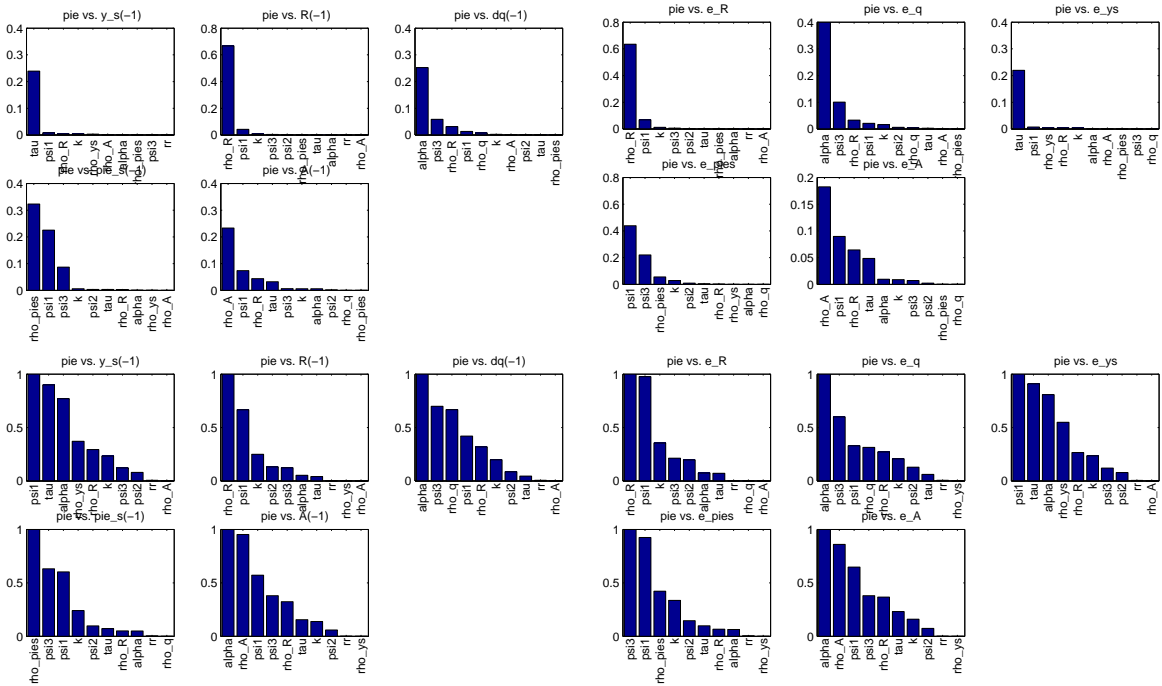


Figure 26: Comparison of ordering of sensitivity indices. There are four groups of graphs, each containing five graphs: First two groups show results for sampling from prior distributions, third and fourth group show results for Morris sampling. Left group always shows results for reduced form coefficients of π against lagged endogenous variables, left group always shows results for for reduced form coefficients of π against exogenous shocks.